Aus der I. Medizinischen Klinik (Institut für Kardiologie, Angiologie,
Pneumologie, Hämostaseologie und internistische Intensivmedizin)
der Medizinischen Fakultät Mannheim
(Direktor: Prof. Dr. med. Martin Borggrefe)

Alpha 1-adrenoceptor signaling contributes to toxic effects of catecholamine on electrical properties in human-induced stem cell-derived cardiomyocytes

Inauguraldissertation
zur Erlangung des medizinischen Doktorgrades
der
Medizinischen Fakultät Mannheim
der Ruprecht-Karls-Universität
zu
Heidelberg

vorgelegt von
Mengying Huang

aus
Sichuan, China
2020

Dekan: Prof. Dr. med. Sergij Goerdt

Referent: Prof. Dr. med. Martin Borggrefe

CONTENTS

ABBREVIATIONS

ACS: Acute coronary syndrome

AP: Action potential

APA: Amplitude of action potential

APD10: Action potential duration at 10% repolarization

APD50: Action potential duration at 50% repolarization

APD90: Action potential duration at 90% repolarization

AR: Adrenoceptor

ARVC: Arrhythmogenic right ventricular cardiomyopathy

Chele: Chelerythrine chloride

Clonidine: Clonidine hydrochloride

CPVT: Catecholaminergic polymorphic ventricular tachycardia

DCFH-DA: 2′,7′-dichlorodihydrofluorescin diacetate

DCFH: Dichlorofluorescin

DCF: Fluorescent dichlorofluorescein

DPI: Diphenyleneiodonium chloride

ECCs: Embryonic carcinoma cells

EF: Ejection fraction

EGCs: Embryonic germ cells

Epi: Epinephrine

ESCs: Embryonic stem cells

FACS: fluorescence-activated cell sorting

GPCR: G-protein coupled receptor

hERG: human ether-a-go-go related gene

$I_{Ca\text{-}L}$: L-Type calcium channel current

I_{Na}: Sodium channel current

$I_{Na\text{-}P}$: Peak sodium channel current

$I_{Na\text{-}L}$: Late sodium channel current

I_{NCX}: Na^{+}/Ca^{2+} exchanger current

I_{kr}: Rapidly activating delayed rectifier potassium channel current

I_{ks}: Slowly activating delayed rectifier potassium channel current

iPSCs: Induced pluripotent stem cells

Iso: Isoprenaline

I_{to}: Transient outward potassium current

LQTs: long QT syndrome

LV: Left ventricle

mRNA: messenger RNA

MYH: Myosin heavy chain

MYL: Myosin light chain

NAC: N-Acetyl-L-cysteine

PCR: Polymerase chain reaction

Pheny: (R)-(-)-Phenylephrine hydrochloride

Phent: Phentolamine methanesulfonate salt

PMA: Phorbol 12-myristate 13-acetate

Prazo: Prazosin hydrochloride

ROS: reactive oxygen species

RP: Resting potential

STEMI: ST-elevation myocardial infarction

TTC: Takotsubo cardiomyopathy

TTS: Takotsubo syndrome

TNNT2: Troponin T2

Vmax: The maximal depolarization velocity of action potential

1. INTRODUCTION

1.1. Takotsubo cardiomyopathy

Takotsubo cardiomyopathy (TTC), which is also called Takotsubo syndrome (TTS) or stress cardiomyopathy, is a stress-associated cardiac disorder. TTS, which often mimicked an acute myocardial infarction with severe left ventricular dysfunction, was first described by Japanese authors in the 1990s [1, 2]. The typical feature is regional left ventricular wall motion abnormality (LVWMA), presenting an unusual appearance of the left ventricle with a narrow neck and apical ballooning during systole [3].The disease was named as ”Takotsubo” because the shape of the left ventricle during systole resembles a Japanese octopus-fishing pot. “Tako” means octopus and “Tsubo” means pot. TTC-patients often display clinical presentations such as chest pain, dyspnoea, syncope, ST-segment elevation, T-wave inversion, regional dyskinesia or akinesia, which are indistinguishable from a myocardial infarction [4, 5]. However, TTC is different from acute coronary syndromes, exhibiting that the coronary angiography usually shows no coronary artery stenosis, the left ventricular dysfunction extends beyond the area covered by a single coronary artery and recovers within days or weeks when appropriately treated [6].

Since the first description of TTS, increasing cases have been recognized worldwide. The prevalence of TTC is estimated to be approximately 1–3% [7, 8] of all and 5–6% [9] of female patients that are suspected with ST-Elevation Myocardial Infarction (STEMI). A study using The Nationwide Inpatient Sample discharge records for the year 2008 reported a prevalence of 0.02% of hospitalized patients in the United States [10]. The recurrence rate of TTC is about 1.8% per-patient year [11]. Most TTC patients, around 90%, are women

between 67–70 years, and about 80% are older than 50 years [11]. Women older than 55 years have a 10-fold higher risk than men [10] .

TTC was originally considered a benign disease [12] . Later studies suggested that the severity of TTC is probably underestimated [3]. Although most patients have a good long-term prognosis, many complications can occur during the acute phase of the disease and the most frequent acute complication is heart failure [4]. About 30% of patients may display life threatening events including pulmonary oedema, cardiogenic shock and ventricular arrhythmias [13]. Long QT interval and torsades de pointes ventricular arrhythmias were frequently observed in affected patients [14]. Apical thrombus formation, cardioembolic stroke, left ventricular free wall rupture, and pericarditis were also reported [15]. Both short-term and long-term mortality are higher than previously estimated [16]. Indeed, it was reported the mortality during the acute phase in hospitalized patients is around 4% to 5%, similar to that of STEMI [17]. Further, it was shown that the mortality in TTC-patients after hospital discharge was higher than that in an aged-matched healthy population although the LV function recovered and no significant coronary disease was detected [18]. The mean in-hospital mortality of TTC was reported as 4.5% [19]. Recently, a study in a large number of patients (n=1750) reported a 30-day mortality of 5.9% and a long-term death rate of 5.6% per patient per year [11].

Although more and more TTC cases are diagnosed due to an increased awareness and recognition of the multiple clinical features of the disease, the pathogenesis of TTC has not been clearly clarified. At present, different mechanisms have been supposed: (1) Multi-vessel coronary artery spasm; (2) Coronary microvascular dysfunction (CMD); (3) Aborted myocardial infarction caused by transient thrombotic occlusion of a long wrap-around left anterior descending artery; (4) Obstruction of left ventricular outflow tract; (5) Cardiac toxicity of plasma catecholamine; (6) Cardiac sympathetic activation; (7)

Switch of ß-adrenoceptor signaling from Gs- to Gi-signaling, leading to ventricular wall motion abnormality; (8) Hypoplastic branching of the coronary arteries in the apical region of the heart, which may contribute to the local ventricular wall motion abnormality; (9) Regional differences in ß-adrenergic receptor density and sympathetic innervations [20]. Among those supposed mechanisms, most are questionable, but the widely accepted central actor contributing to the pathogenesis of TTC is the catecholamine excess, either from circulation or from local sympathetic nerve endings in the heart. Most patients with TTC experienced various stresses before an attack, such as the unexpected death of a relative or lover, the suppression of terror, the occurrence of a natural disaster, or severe physical stress, which often leads to emotional or psychological stress [6]. Therefore, TTC is also called “Heart Broken Syndrome” [3]. Recently, it was shown that TTC can also happen after a positive life event. So the name “happy heart syndrome” was also suggested for TTC [21]. Moreover, tests showed that serum catecholamine levels were elevated in more than 70% of TTC patients [22]. Strikingly, researchers found that plasma levels of catecholamines (adrenaline, norepinephrine, and dopamine) were several times higher in patients with TTC than in patients with STEMI (ST-Elevation Myocardial Infarction) during the acute phase, meanwhile myocardial levels of catecholamines also increased, and both levels stayed significantly high even one week after the onset of symptoms [22]. In addition, recent clinical cases have showed that some patients developed TTC after being injected subcutaneously with a large dose of epinephrine [23-26]. Studies in murine model have shown that injected high concentrations of epinephrine can produce reversible apical LV ballooning expansion and abnormal contractions similar to those in patients with TTC [27]. Taking together, increasing evidences indicate a contribution of catecholamine excess to TTC pathogenesis.

Since beta-adrenoceptors play important roles for heart function and TTC is related with catecholamine excess, administration of beta-blockers is a logical pharmacotherapy for TTC-treatment. Indeed, beta-blockers are commonly prescribed for some TTC-patients. Besides beta-blockers, treatments for TTC often contained emotional or physical stress relief, application of anticoagulants, angiotensin-converting enzyme inhibitors or aldosterone receptor blockers or angiotensin receptor blockers and statins in clinical practice [28, 29]. A beta-blocker may protect cardiomyocytes from toxic effects of high concentration of catecholamine. Actually, TTC-patients who were treated with conventional beta-blockers upon admission had a 59.6% relapse after discharge, and most of them received beta1-selective compounds (84.6%) [30]. Strikingly, a study reported that application of beta-blocker during the acute phase of TTC showed no benefits regarding the in-hospital mortality in patients with or without left ventricular outflow tract obstruction [31]. Another study reported that the application of beta-blockers in TTC-patients after discharge showed no beneficial effect on mortality after 1 year of follow-up [11]. Furthermore, no benefit of beta-blockers in preventing recurrence of TTC was detected in two meta-analyses [19, 32]. All of these evidences may suggest that mechanisms other than beta-receptor mediated signaling contribute also to the pathogenesis of TTC. Of note, previously reported studies focused on roles of the beta-adrenoceptor related signaling for the pathogenesis of TTC. Studies on non-beta-adrenoceptor signaling for occurrence of TTC remain spars.

It is known that alpha-adrenoceptors exist in cardiomyocytes [33] . Animal experiments show that direct activation of cardiac alpha- and beta-adrenoceptors induced angina-like change (ST segment elevation) [34]. A study in rats showed that the alpha 1-receptor agonist phenylephrine induced TTC-like heart dysfunctions [35]. Another study demonstrated that when rats were exposed to emotional stress evoked by immobilization (IMO)

for 30 minutes and then injected with the α2-AR agonist xylazine, the cardiac ejection fraction and the movement of the anterior wall were suppressed, whereas posterior wall movement was preserved, similar to TTC-phenotype [36], suggesting contribution of alpha-adrenoceptor signaling to occurrence of TTC. In addition, studies in rats showed that combining prazosin with metoprolol or amoxolol can eliminate stress-induced tachycardia and ST-segment elevation, which shows that simultaneous inhibition of α1- and β1-adrenergic receptors have a certain effect on the suppression of stress cardiomyopathy [34, 37]. It is a pity that all the studies that showed a contribution to alpha-adrenoceptor to TTC did not clarify which signaling or mechanism mediated the contribution of an alpha-adrenoceptor activation to the pathogenesis or arrhythmogenesis.

Moreover, in a case of catecholamine-induced myocardial damage, the patient treated with beta-blocker propranolol worsened symptoms and even developed seriously heart failure, but re-administration of alpha-blockers relieved the symptoms [38]. Given the findings from animal and human studies, treatment with a combined alpha- and beta-blocker might be reasonable for some TTC-patients [39]. Taken all together, data suggest that α-adrenoceptor signaling can take part in TTC-pathogenesis and blocking α-adrenoceptors may have therapeutic benefits for TTC-patients. However, studies on α-adrenoceptor mediated signaling in human cardiomyocytes from TTC-patients or in the setting of TTC are still lacking. The importance of alpha-adrenoceptor signaling for LQTs and occurrence of arrhythmias under circumstances of TTC is still unknown.

1.2. Induced pluripotent stem cells

Embryonic stem (ES) cells derived from the inner cell mass of mammalian blastocysts not only have the ability to grow indefinitely but also maintain pluripotency, and can differentiate into cells of all three germ layers [40, 41].

Therefore, in the past, people often used ES cells to build various disease models, further understand the disease mechanism, screen effective and safe drugs, and treat various diseases and injuries [41]. However, the ethical controversy over the use of human embryos and tissue rejection after patient transplantation limited the use of human ES cells. Generating pluripotent cells directly from patient-specific somatic cells can solve these problems [42]. In 2006, Takahashi K and Yamanaka S successfully generated pluripotent stem cells from mouse adult fibroblasts through overexpression of identified factors [42]. They introduced four factors Octct3 / 4, Sox2, c-Myc and Klf4 (also called Yamanaka factors) under ES cell culture conditions, and successfully induced adult fibroblasts to differentiate into pluripotent stem cells. These cells, called iPS (induced pluripotent stem cells), have the morphological and growth characteristics of ES cells and express ES cell marker genes [42].

In 2007, with the same four factors: Oct3/4, Sox2, Klf4, and c-Myc, Takahashi et al successfully reprogrammed adult human dermal fibroblasts (HDF) from facial dermis of 36-year-old Caucasian female to pluripotent stem cells (first human iPS cell) [43]. Further testing revealed that human iPS cells were similar to human embryonic stem (ES) cells. Each induced pluripotent cell had a morphology and karyotype similar to that of human ES cells [44]. The epigenetic status and telomerase activity of each human induced pluripotent cell-specific gene are similar to that of human embryonic stem (ES) cells [43, 44]. Furthermore, in vitro, these cells also could differentiate into cell types of the three germ layers as ES cells.

In 2008, Genta Narazaki and colleagues successfully differentiated mouse iPSCs into cardiomyocytes [45] . Since then, numerous studies using iPS cell-derived cardiomyocytes (iPSC-CMs) have been published, demonstrating that iPSC-CMs possess features similar to adult cardiomyocytes. Importantly, the human iPSC-CMs (hiPSC-CMs) have been shown to have the ability to

recapitulate phenotypic features of heart diseases such as long- and short-QT syndromes [46, 47], Brugada-syndrome [48], arrhythmogenic right ventricular cardiomyopathy (ARVC) [49], catecholaminergic polymorphic ventricular tachycardia (CPVT) [50], hypertrophic and dilated cardiomyopathy [51]. Therefore, hiPSC-CMs provide a good platform for studies on human cardiomyocytes, including physiology, pathophysiology and drug screening.

1.3. Takotsubo cardiomyopathy disease models

In the past, many studies have used a single dose of the selective β-adrenergic agonist isoprenaline (Iso) to induce a Takotsubo-like (TTC-like) model in mice [52]. But isoprenaline is only an agonist of the β receptor, and it is very limited to study the effects of other adrenoceptors on TTC-pathogenesis. Redfors et al. showed that not only isoprenaline but also epinephrine could induce TTC-like cardiac dysfunction in rats [35]. Paur et al established an in vivo animal model of epinephrine-induced TTC that recapitulated the apical inhibition of the heart contraction and the reversibility of this cardiac inhibition [27].

Although TTC models have been successfully established in animals, animal models are not ideal for simulating human diseases. The differences between animal and human being lead to limitations of animal studies. Human adult cardiomyocytes are ideal for studies on human cardiac disorders. However, the limited availability of human cardiomyocytes, especially the ventricular cardiomyocytes, is a major obstacle for studying human heart disease including TTC. Therefore, hiPSCs provide an opportunity to establish cellular models of human cardiac disorders. Recently, our group successfully generated hiPSC-CMs from healthy donors and investigated the toxic effects of high concentration of isoprenaline mimicking the setting of TTC [34]. Another group successfully generated hiPSC-CMs from two TTC-patients and demonstrated that hiPSC-CMs from TTC-patients showed higher sensitivity to

isoprenaline challenge when compared with hiPSC-CMs from healthy donors [53]. Both studies indicate that TTC-phenotypic features were successfully modeled by hiPSC-CMs and this model can be useful for studying pathogenesis of TTC.

In summary, so far available data suggest that alpha-adrenoceptors may contribute to pathogenesis of TTC, but the detailed intracellular signaling that mediated the effects of alpha-receptor activation in the setting of TTC (high concentration of catecholamine) has not been clarified. The roles of alpha-receptor signaling for long QT interval and arrhythmias caused by high and toxic concentration of catecholamine and the underlying ionic mechanisms are still unknown.

1.4. Aims of the study

Based on previous data demonstrating that (1) activation of sympathetic nerves and catecholamine excess play an important role for pathogenesis of TTC and (2) both α-and β-adrenoceptor blockers attenuated TTC phenotypic changes, we hypothesize that (1) α-adrenoceptor signaling may contribute to ion channel dysfunctions caused by toxic effects of high concentration of catecholamine, (2) α-adrenoceptor signaling may contribute to the long QT interval and occurrence of arrhythmias in the setting of high concentration of catecholamine.

The purposes of this study were to use hiPSC-CMs for: (1) examining the involvement of α-adrenoceptor signaling in alterations of ion channel functions and action potentials caused by toxic concentration of catecholamine, (2) assessing possible roles of the α-adrenoceptor signaling for the occurrence of arrhythmias caused by toxic concentration of catecholamine and (3) exploring possible mechanisms underlying the α-adrenoceptor mediated changes in the presence of toxic concentration of catecholamine.

2. METHODS AND MATERIALS

2.1. Ethics statement

The skin biopsies from 3 healthy donors were obtained with written informed consent. The study was approved by the Ethics Committee of Medical Faculty Mannheim, University of Heidelberg (approval number: 2018-565N-MA) and conducted in accordance with the Helsinki Declaration of 1975 (https://www.wma.net/what-we-do/medical-ethics/declaration-of-helsinki/), revised in 2013.

2.2. Study design

To investigate possible roles of α-adrenoceptor signaling in arrhythmogenesis in TTC, the following experiments were designed (Figure 1):

1) Assessment of toxic effects of high concentration of epinephrine (500 μM) on action potentials and occurrence of arrhythmias in hiPSC-CMs.

2) Assessment of the involvement of α-adrenoceptor signaling in epinephrine effects by application of different α-adrenoceptor blockers and agonists.

3) Assessment of roles of activation of α-adrenoceptor signaling on currents and expression levels of ion channels responsible for abnormal action potentials and arrhythmias.

4) Identifying signaling factors responsible for the effects induced by α-adrenoceptor activation.

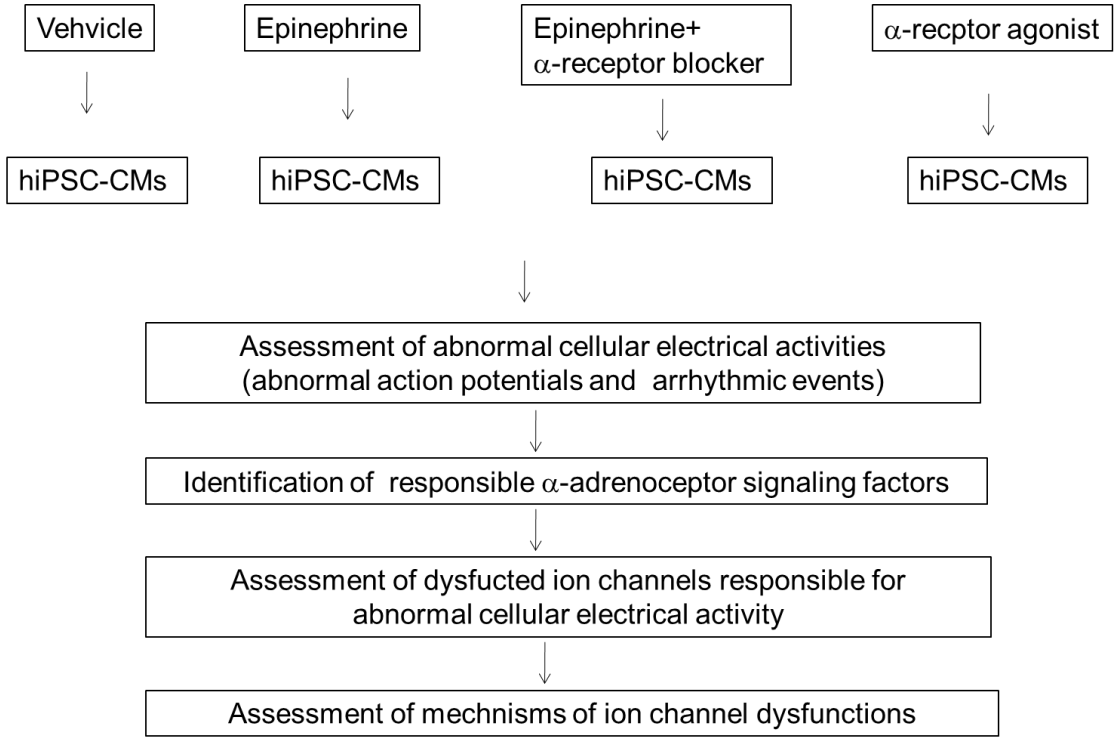

Figure 1. Study design of experiments.

2.3. Generation of hiPSC-CMs

Skin fibroblasts from three healthy donors (here named as D1, D2 and D3) were used for generation of iPS cells. D1 and D3 are female, while D2 is male. The generation of iPS cells from the fibroblasts was performed by Dr. Cyganek´s group (the Stem Cell Unit, Clinic for Cardiology and Pneumology, University Medical Center Göttingen, Germany) and described in our previous studies[54-56].

The generated hiPS cell (hiPSC) lines from the three healthy donors were differentiated into cardiomyocytes (hiPSC-CMs) as described in our previous studies [54-56]. Briefly, culture dishes and wells were coated with Matrigel (Corning). The culture medium of hiPSCs was TeSR-E8 (Stemcell Technologies) and the cardiac medium for hiPSC-CMs was RPMI1640 Glutamax (Life Technologies) consisting of 1% sodium pyruvate, 1% Penicillin/Streptomycin, ascorbic acid (Sigma Aldrich) and B27 (Life

Technologies). During the first two weeks, CHIR99021 (Stemgent), BMP-4 (R&DSystems), FGF-2 (MiltenyiBiotec), Activin A (R&D Systems), and IWP-4 (Stemgent) were added at different times to induce the cells to differentiate into hiPSC-CMs. During the third week the selection medium which contained sodium lactate (Sigma, Germany) and RPMI medium without glucose and glutamine (WKS, Germany) was used to select cardiomyocytes. At 30 to 60 days of differentiation, the cells were cultured with basic cardiac medium. After 60 days of differentiation, the cardiomyocytes were dissociated from 6 well plates and used for PCR, immunofluorescence, flow cytometry analysis, or plated on Matrigel-coated 3.5 cm petri dishes as single cells for patch clamp test.

The protocols for differentiation of iPS cells into cardiomyocytes are from the lab of Dr. Cyganek and Prof. Zimmermann in University of Göttingen. Using the same protocols, three clones of each cell line were alternately differentiated into hiPSC-CMs and data from all the three clones were combined for a cell line. At least 2 individual differentiation experiments of each clone were used for data analysis.

After differentiation, the differentiation efficiency of iPSC-CMs was determined by flow cytometry analysis using an antibody against cardiac cTnT (TNNT2). A successful differentiation resulted in a purity of more than 90% of cardiomyocytes. Differentiation efficiency was also determined by observation of contracting cells and only cultures covered with greater than 90% contracting areas were used for further experiments. Importantly, no significant difference in the differentiation efficiency was detected among different cell lines.

The success of the differentiation of cardiomyocytes was confirmed by spontaneous cell beating, the expression of cardiac markers like alpha-actinin

and cTnT and the cardiac action potentials, which are different from that in other types of cells including smooth and skeletal muscle cells.

2.4. Polymerase chain reaction assays

Quantitative polymerase chain reaction assays (qPCR) was performed following the protocol and using the RNeasy mini kit (Qiagen, Hilden, Germany) to extract total RNA. The extracted RNA (10 μl) was reverse transcribed into cDNA using High-Capacity cDNA Reverse Transcription Kit (Thermo Fisher) on a Stratagene MX 3005P Real-Time Cycler (Stratagene, USA). Real-time quantitative PCR analysis was performed in the presence of sense and antisense primers (each 400 nM) using a quantitative SYBR Green PCR kit (SibirRox Hot Mastermix, Bioron, Germany) on StepOnePlus Real-Time PCR Systems (Thermo Fisher).

The relative mRNA expression level is calculated as follows: According to the threshold cycle (CT), the ΔΔCT method is used to calculate the mRNA expression of the target gene relative to the housekeeping gene GAPDH in a sample of treated or untreated (control) cells, as a fold change = 2-Δ (ΔCT), where ΔCT = CTgene of interest-CTGAPDH and Δ (ΔCT) = ΔCT treated-ΔCT control [57]. To ensure reproducibility, the control and treatment groups were repeated three times independently. Each sample was given into two wells as a technical replicate to repeat the measurements. Statistics using mean ± SEM method.

2.5. Patch-clamp

The hiPSC-CMs on day 60 to day 80 were washed with PBS (w / o Ca, Mg) and incubated with 0.05% Trypsin-EDTA (Life Technologies) for 10 min at 37 °C. Then RPMI medium + 10% FBS was added and pipetted up and down to obtain single cells. The cell suspension was centrifuged at 250 × g for 4 min at room temperature, supernatant was aspirated and cells were resuspended

with SF (cardiac medium + B27 + ASC). For patch-clamp experiments, the density of cells in the dish was 2-4 × 10^4.

We used standard whole-cell patch-clamp recording techniques (Figure 2) to record different ion channel currents including the sodium (I_{Na}), L-type calcium ($I_{Ca\text{-}L}$), transient outward potassium (I_{to}), rapidly activating delayed rectifier potassium (I_{Kr}) current and action potential (AP) at room temperature. Furthermore, we used some specific channel blockers and different solutions or protocols to isolate a type from other types of ion channel currents. To minimize the influence of the rundown of recorded currents on the experimental results, we usually started the recordings after the current or AP was stabilized (3-5 minutes after the whole cell configuration was established). The patch electrode used for AP and current measurements was pulled from borosilicate glass capillary (MTW 150F; World Precision Instruments, Sarasota, FL) by the DMZ universal puller (Zeitz-Instrumente Vertriebs GmbH, Martin Reed, Germany) and filled with pre-filtered pipette solution (see below). The pipette resistance range for measuring currents was 2–4 MΩ and for measuring APs was 4-5 MΩ.

After the patch pipette was carefully moved on the cell membrane by a micromanipulator (Figure 2A-B), a slight suction (negative pressure) was given to obtain high-resistance (Giga-Ohm) seal between cell membrane and the pipette wall (also called Giga-seal, Figure 2C), and then further suction was applied to rapture the membrane that was sucked into the pipette and establish a whole cell configuration (Figure 2D). Before the membrane capacitance was compensated, a voltage pulse of 10 ms from -80 mV to -85 mV was given to record the capacitance transient current. Signals were acquired at 10 kHz and filtered at 2 kHz with the EPC10 Patch-master digitizer hardware (HEKA Germany) and Fit-master software (HEKA Germany). The measured capacitance current was used to calculate the cell membrane

capacitance in pF by dividing the area under capacitance current by 5. All the measured ion channel currents were normalized to the membrane capacitance to gain current densities in pA/pF. The current density is plotted against the respective voltages to produce a current-voltage (I-V) relationship curves.

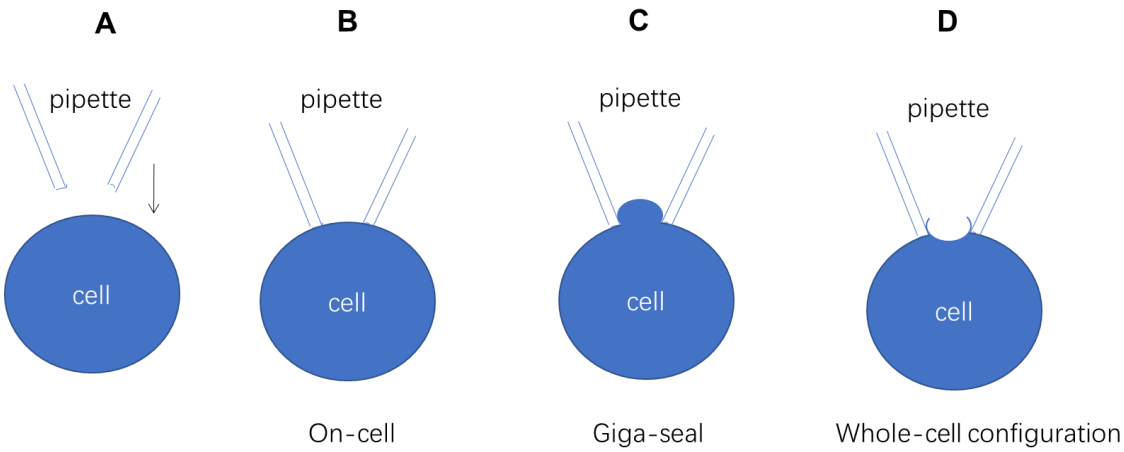

Figure 2. Establishment of whole-cell configuration of patch clamp recordings.

APs were measured in current-clamp mode (CC-mode). Spontaneous APs were recorded at CC-mode without stimulations. The frequency and arrhythmic events such as irregular beatings, early after depolarizations, delayed after depolarizations and trigger activities were analyzed if they occurred during recordings.

For recording APs paced at a fixed frequency, a short current pulse (2 ms, 1nA) was applied at 1 Hz to trigger the action potentials. The AP parameters including the resting potential (RP), AP amplitude (APA), the maximal velocity of depolarization (Vmax), the AP duration at 10% repolarization (APD10), the AP duration at 50% repolarization (APD50) and the AP duration at 90% repolarization (APD90) were analyzed (Figure 3).

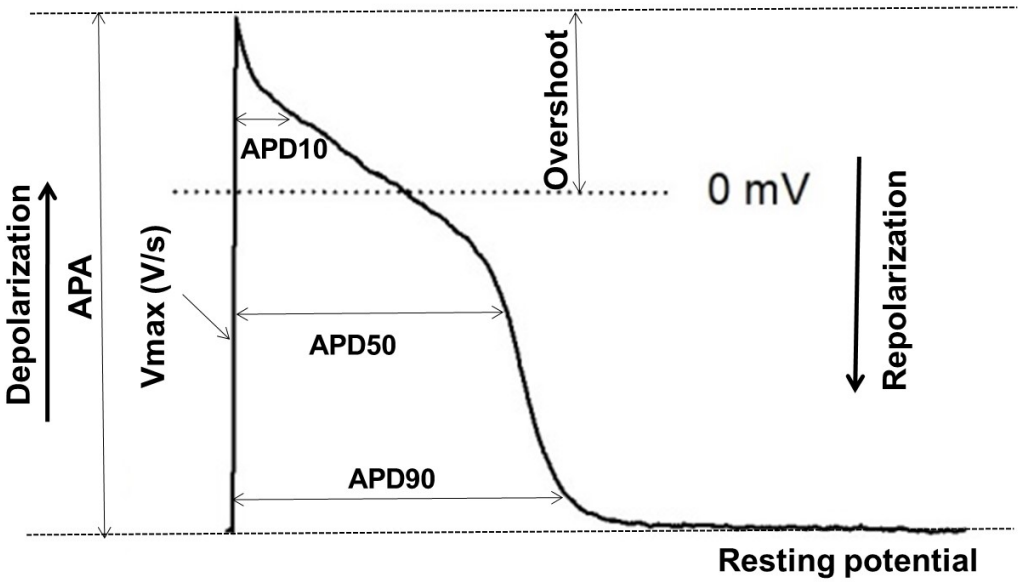

Figure 3. Analysis of action potential parameters.

The extracellular solution for recording APs and transient outward potassium channel (I_{to}) currents contained 127 mmol/L NaCl, 5.9 mmol/L KCl, 2.4 mmol/L $CaCl_2$, 1.2 mmol/L $MgCl_2$, 11 mmol/L glucose, and 10 mmol/L HEPES. The pH value was adjusted to 7.4 with NaOH. 1 umol/L nifedipine, 1 umol/L E-4031, and10 umol/L TTX were added to block the $I_{Ca\text{-}L}$, I_{Kr}, and I_{Na}, respectively when transient outward potassium current (I_{to}) was recorded. The intracellular solution comprised 6 mmol/L NaCl, 126 mmol/L KCl, 1.2 mmol/L $MgCl_2$, 5 mmol/L EGTA, 11 mmol/L glucose, 10 mmol/L HEPES and 1 mmol/L Mg-ATP. The pH value was adjusted to 7.2 with KOH.

The extracellular solution for rapidly activating delayed rectifier potassium (I_{Kr}) contained 135 mmol/L CsCl, 1 mmol/L $MgCl_2$, 10 mmol/L glucose, 10 mmol/L

HEPES. The pH value was adjusted to 7.4 with CsOH. The intracellular solution was the same as the extracellular solution.

The extracellular solution for peak sodium current measurements contained 20 mmol/L NaCl, 130 mmol/L CsCl, 1.8 mmol/L $CaCl_2$, 1 mmol/L $MgCl_2$, 10 mmol/L Hepes, 10 mmol/L glucose, 0.001 mmol/L nifedipine. The pH value was adjusted to 7.4 with CsOH. The extracellular solution for late sodium current measurements contained 135 mmol/L NaCl, 20 mmol/L CsCl, 1.8 mmol/L $CaCl_2$, 1 mmol/L $MgCl_2$, 10 mmol/L Hepes, 10 mmol/L glucose, 0.001 mmol/L nifedipine, pH 7.4 (CsOH). The intracellular solution for peak and late sodium current contained 10 mmol/L NaCl, 135 mmol/L CsCl, 2 mmol/L $CaCl_2$, 3 mmol/L Mg-ATP, 5 mmol/L EGTA, 10 mmol/L HEPES, pH 7.2 (CsOH).

The extracellular solution for L-type calcium channel current ($I_{Ca\text{-}L}$) measurements contained 140 mmol/L TEA-Cl, 5 mmol/L $CaCl_2$, 1 mmol/L $MgCl_2$, 10 mmol/L HEPES, 10 mmol/L glucose, pH 7.4 (CsOH). The intracellular solution contained 10 mmol/L NaCl, 135 mmol/L CsCl, 2 mmol/L $CaCl_2$, 3 mmol/L Mg-ATP, 5 mmol/L EGTA, 10 mmol/L HEPES, pH 7.2 (CsOH).

The extracellular solution for Na^+/Ca^{2+} exchanger current (I_{NCX}) measurements contained 135 mmol/L NaCl, 10 mmol/L CsCl, 2 mmol/L $CaCl_2$, 1 mmol/L $MgCl_2$, 10 mmol/L HEPES, 10 mmol/L glucose, 0.01 mmol/L nifedipine, 0.1 mmol/L niflumic acid, 0.05 mmol/L lidocaine, and 0.02 mmol/L dihydroouabain (pH 7.4 (CsOH)). The intracellular solution contained 1 mmol/L $MgCl_2$, 115 mmol/L CsCl, 1 mmol/L $CaCl_2$, 10 mmol/L NaCl, 3 mmol/L Mg-ATP, and 5 mmol/L EGTA, 20 mmol/L TEA-Cl, 10 mmol/L HEPES, pH 7.2 (CsOH).

2.6. Flow cytometry

The ROS production in hiPSC-CMs was evaluated by 2′,7′-Dichlorofluorescin diacetate (DCFH-DA, sigma) method according to the ROS assay kit

instructions. DCFH-DA is a non-polar fluorescence probe that can penetrate cell membranes, where it is converted into DCFH and then detected by flow cytometry. The cardiomyocytes were incubated with 300 µl (150 U) collagenase CLS I (Worthington, Germany) for 40 min at 37 °C, and then washed with PBS and incubated with 0.05% Trypsin-EDTA (Life Technologies) for 2-4 min at 37 °C. After adding RPMI medium containing 10% FBS, these cells were centrifuged at 250 × g for 4 min at room temperature. Next the supernatant was discarded and the cells was resuspended in basic culture medium. The cells were plated into the 15ml tubes at a density of 1×10^4 cells/tubes and incubated with 10 µM DCFH-DA at 37°C for 30 minutes in the dark. After the cells were washed 3 times with PBS, they were measured on BD FACSCanto™ II (Becton Dickinson, Heidelberg, Germany). Analysis was performed using a quantitative method via BD FACS Diva software (Version 8.0.1).

2.7. Immunofluorescence (IF) staining

The cardiomyocytes were incubated with 0.05% Trypsin-EDTA (Life Technologies) for 2-4 min at 37 °C. After adding RPMI medium containing 10% FBS, these cells were centrifuged at 250 × g for 4 min at room temperature. Next, the supernatant was discarded and the cells was resuspended in basic culture medium and pipetted onto culture slides (FALCON 354114). After slides stayed overnight, they were washed with PBS 2-3 times, and then fixed with 4% paraformaldehyde (Sigma) at RT for 20 min. After washed with PBS 2-3 times, cells were permeabilized with 0.1% Triton-X100 (Carl Roth) for 10 min. Then they were washed with PBS 2-3 times and blocked with 5% bovine serum albumin (BSA; Sigma-Aldrich) in PBS at 4°C for 1 h. Primary antibodies were applied in 5% BSA overnight at 4°C. Cells were then washed with PBS and incubated for 1 h at room temperature with corresponding secondary antibodies conjugated to Alexa Fluor 488 or 642 (1:200). Cells were then

washed with PBS, incubated with DAPI (Biozol) for 10 min at RT in the dark. Images were collected using the confocal microscope TCS SP-8 upright (Leica, Germany) with Plan-Apochromat 40×/0.6 objective.

2.8. Materials (primers, antibodies, kits and substances)

Table 1. Reagents and substances.

Kits and substances	Company
RNeasy Mini Kit (250)	Qiagen
High-Capacity cDNA Reverse Transcription Kit	Thermo Fisher
SibirRoxHot Master Mix, ROX 0.1μM	Bioron
VECTASHIELD with DAPI 10 ml	Biozol
Phentolamine methanesulfonate salt	Sigma
N-Acetyl-L-cysteine	Sigma
2′,7′-Dichlorofluorescin diacetate	Sigma
Clonidine hydrochloride	Sigma
(R)-(−)-Phenylephrine hydrochloride	Sigma
H_2O_2 (30%)	Merck
(±)-Epinephrine hydrochloride	Sigma
Chelerythrine chloride	Sigma
Prazosin hydrochloride	Sigma

Table 2. Primer sequences for real-time polymerase chain reaction (PCR).

Primer	Company
Hs_ADRA1A_1_SG QuantiTect Primer Assay	Qiagen
Hs_ADRA2A_1_SG QuantiTect Primer Assay	Qiagen
Hs_CACNA1C_1_SG QuantiTect Primer Assay	Qiagen
Hs_SCN5A_1_SG QuantiTect Primer Assay	Qiagen

Hs_SCN10A_1_SG QuantiTect Primer Assay	Qiagen
Hs_KCNH2_2_SG QuantiTect Primer Assay	Qiagen
Hs_KCNQ1_1_SG QuantiTect Primer Assay	Qiagen
Hs_KCND3_1_SG QuantiTect Primer Assay	Qiagen
Hs_SLC8A1_1_SG QuantiTect Primer Assay	Qiagen
Hs_GAPDH_1_SG QuantiTect Primer Assay	Qiagen
G protein alpha S / GNAS qPCR Primer Pairs, Human	Sino Biological Inc.

Primer	Direction	Sequence	Size (bp)
GNAI2	forward	5'-CTTGTCTGAGATGCTGGTAATGG-3'	23
	reverse	5'-CTCCCTGTAAACATTTGGACTTG-3'	23
GNAQ	forward	5'-GACTACTTCCCAGAATATGATGGAC-3'	25
	reverse	5'-GGTTCAGGTCCACGAACATC-3'	20
GNA11	forward	5'-GATCCTCTACAAGTACGAGCAGAAC-3'	25
	reverse	5'-ACTGATGCTCGAAGGTGGTC-3'	20

Table 3. Antibody for Immunofluorescence (IF) staining.

Antibody	Company
Alexa Fluor® 647 Mouse Anti-Cardiac Troponin T	BD Biosciences
Anti-alpha 1 Adrenergic Receptor/ADRA1 antibody	Abcam
Goat anti-Mouse IgG (H+L) Highly Cross-Adsorbed Secondary Antibody, Alexa Fluor Plus 488	Thermofisher
Chromeo™ 642 Goat anti-Rabbit IgG	Active Motif
Anti-Cardiac Troponin T antibody	Abcam

2.9. Statistics

All data are shown as mean ± SEM and were analyzed using SigmaPlot 14.0 (Systat GmbH, Germany). By analyzing the data with the Kolmogorov Smirnov test, it was decided whether parametric or non-parametric tests were used for analysis. The t-test was used for comparisons of two independent groups with normal distribution. For parametric data one-way ANOVA with Holm-Sidak post-test for multiple comparisons (all treated groups versus control) were performed. For non-parametric data the Kruskal-Wallis test with Dunn's multiple comparisons post-test was used. To compare categorical variables, the Fisher-test was used. $P < 0.05$ (two-tailed) was considered significant.

3. RESULTS

3.1. Characterization of hiPSC-CMs

Cardiomyocytes generated from hiPS-cells that were derived from skin fibroblasts of three healthy donors (D1, D2, D3) were used for the study. D1 was used for the majority of the study. D2 and D3 were used for examining the individual variability in results. The successful generation of hiPSC-CMs from hiPSCs was confirmed by qPCR or immunostaining and FACS analysis of the expression of cardiac markers and showed in our recent publications [49]. In the current study, the cardiac marker cTnT (TNNT2) was examined again by immunostaining (Figure 4C) and FACS (Figure 10B). These data together with the cell beating and action potentials with cardiac morphology indicate the successful differentiation of cardiomyocytes.

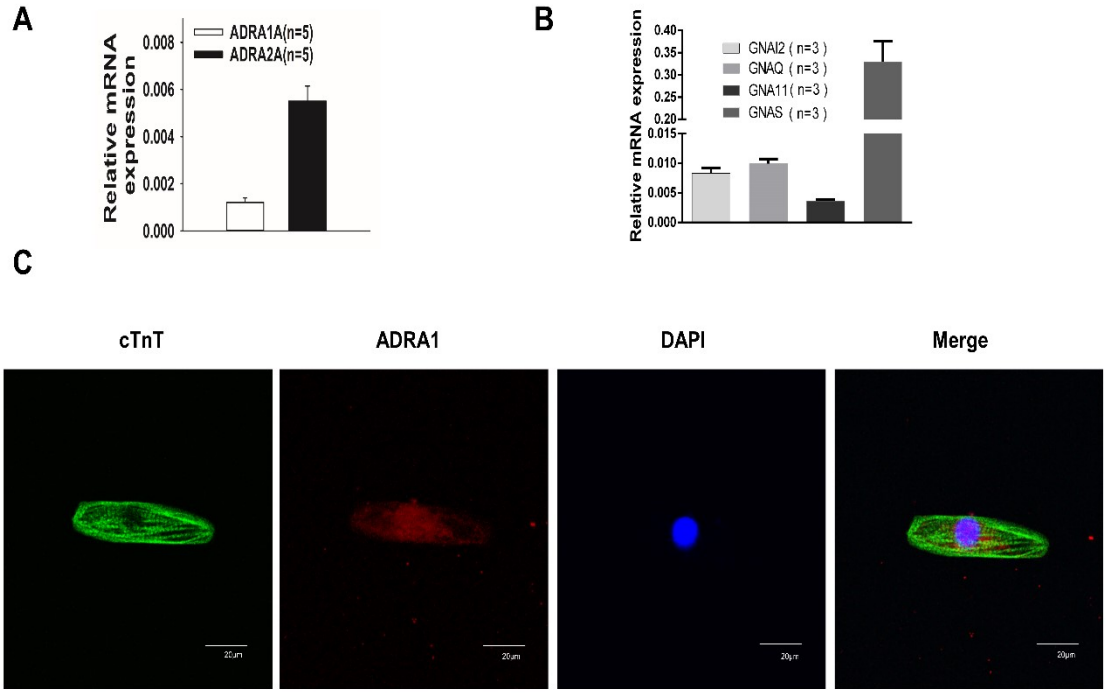

Figure 4. PCR assay and immunofluorescence of alpha-adrenoceptor and G protein expression. mRNA levels are normalized with GAPDH as a housekeeping gene. (A) Expression level of mRNA for α1 (ADRA1A) and α2 (ADRA2A) adrenoceptors in hiPSC-CMs. (B) Expression level of mRNA for Gs (GNAS), Gi (GNAI2), Gq (GNAQ and GNA11) in hiPSC-CMs. (C) Confocal images of immunofluorescence staining of cTnT (green) and ADRA1 (red). The nucleus was stained by DAPI (blue). The “n” numbers represent experimental numbers. Scale bars: 20 μm. cTnT: cardiac muscle troponin T, a marker of cardiomyocyte.

3.2. Alpha-adrenoceptor and G protein expression in hiPSC-CMs

To determine whether the α-adrenergic receptor and G protein are expressed in the differentiated hiPSC-CMs, we analyzed the mRNA levels of two α-adrenergic receptors (ADRA1A, ADRA2A) and three groups of G proteins.

Our data confirmed that the ADRA1A and ADRA2A α-adrenergic receptor isoforms exist in hiPSC-CMs (Figure 4A). Differential expression of adrenergic receptor associated proteins including Gq, Gi and Gs proteins could also be detected in differentiated hiPSC-CMs (Figure 4B). Furthermore, the localization of ADRA1A in 60- to 80-day-old hiPSC-CMs were analyzed using immunocytochemistry. ADRA1A is widely distributed but predominantly on the microtubule network and near cell membrane and nucleus (Figure 4C).

3.3. The α-adrenoceptor activation contributed to effects of epinephrine on ion channel expression

To examine whether α-adrenoceptors play important roles for ion channel dysfunctions in the setting of TTC, we first checked the expression profile of ion channels related to changing of the action potentials in hiPSC-CMs challenged by high concentration (500 μM) epinephrine (Epi). At the same time, we analyzed the effects of an α-adrenoceptor blocker against the effects of Epi on ion channel expression levels (Figure 5).The expression levels of CACNA1C (coding L-type calcium channel), SCN10A (coding Nav1.8 sodium channel) and SLC8A1 (coding Na^+/Ca^{2+}-exchanger, NCX1) genes were elevated by Epi (Figure 5 A-C), but the expression of SCN5A (coding Nav1.5 sodium channel), KCNH2 (coding I_{Kr}, also called HERG channel) and KCND3 (coding I_{to} channel, Kv4.3) gene was reduced by Epi (Figure 5 D-F). Epi did not influence the expression level of KCNQ1 (coding I_{Ks} channels) (Figure 5 G). The α-adrenoceptor blocker phentolamine (500 μM) prevented the Epi-effects on gene expression levels (Figure 5), suggesting the α-adrenoceptor signaling may contribute to ion channel dysfunctions in the setting of TTC.

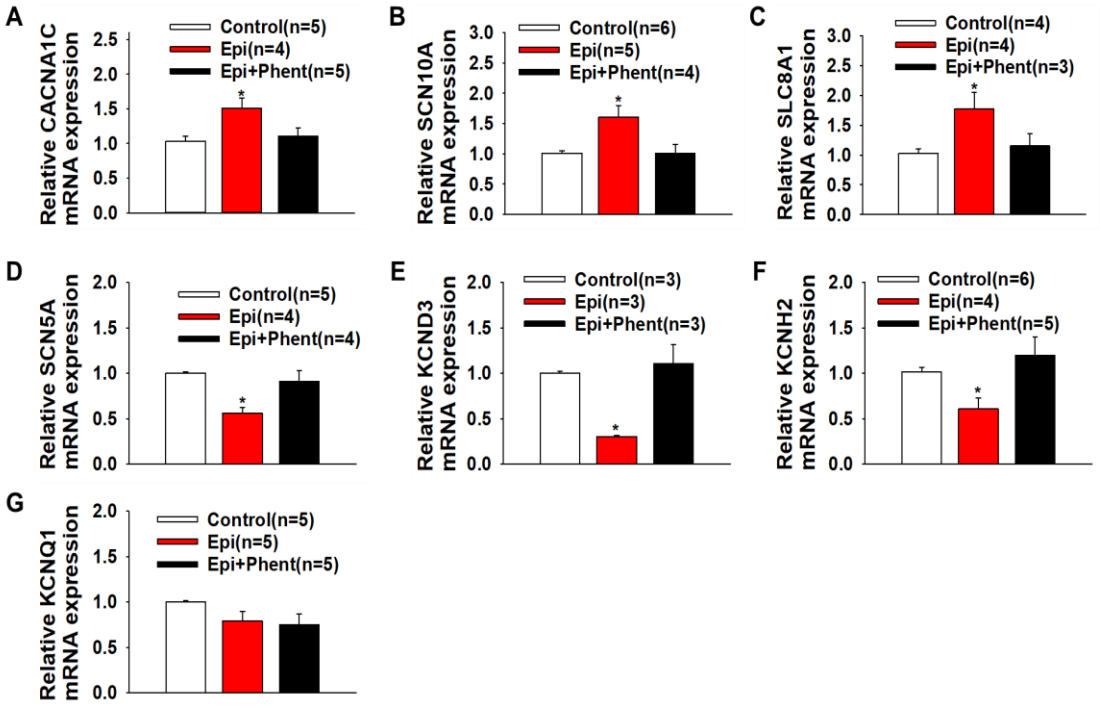

Figure 5. Activation of alpha-adrenoceptor changed ion channel expression levels. hiPSC-CMs were treated for 1 h with either vehicle (Control) or 500 μM epinephrine (Epi) or epinephrine plus 500 μM phentolamine (Epi+Phent). qPCR analysis was performed to measure the expression levels of ion channels. (A) Mean values of L-type calcium channel (CACNA1C) expression. (B) Mean values of sodium channel (SCN10A) expression. (C) Mean values of Na^+/Ca^{2+} exchanger (SLC8A1) expression. (D) Mean values of cardiac sodium channel (SCN5A) expression. (E) Mean values of transient outward K channel (KCND3, I_{to}) expression. (F) Mean values of rapidly activating delayed rectifier K (KCNH2, I_{Kr}) channel expression. (G) Mean values of slowly activating delayed rectifier K (KCNQ1, I_{Ks}) channel expression. “n” represents experimental numbers (biological replicates). *p<0.05 versus Control according to the analysis of one-way ANOVA with Holm-Sidak post-test.

3.4. The α-adrenoceptor activation contributed to toxic effects of epinephrine on action potentials

To evaluate the contributions of α-adrenoceptors to the toxic effects of catecholamine excess on cellular electrophysiology, we assessed the effects of epinephrine (500 μM,1 hour) on the action potential (AP) properties of cardiomyocytes. Epinephrine treatment did not change the RP (resting potential) and APA (amplitude of action potential), but reduced Vmax (maximal upstroke velocity) and prolonged APD10 (the action potential duration at 10% repolarization) from 11.32 ± 0.16 ms to 13.09 ±0.49 ms, APD50 (the action potential duration at 50% repolarization) from 128.26±28.40 ms to 453.20+56.31 ms and APD90 (the action potential duration at 90% repolarization) from 277.91±36.92 ms to 615.37± 62.79 ms, respectively (Figure 6). After treatment with phentolamine (Phent, 500 μM, a non-selective alpha receptor antagonist) in the presence of epinephrine, the effects of epinephrine were reversed (Figure 6A-E). Phentolamine alone had no effect on AP characteristic of hiPSC-CMs (Figure 6). These results indicate that α-adrenoceptor activation plays an important role in Epi-effects on APs.

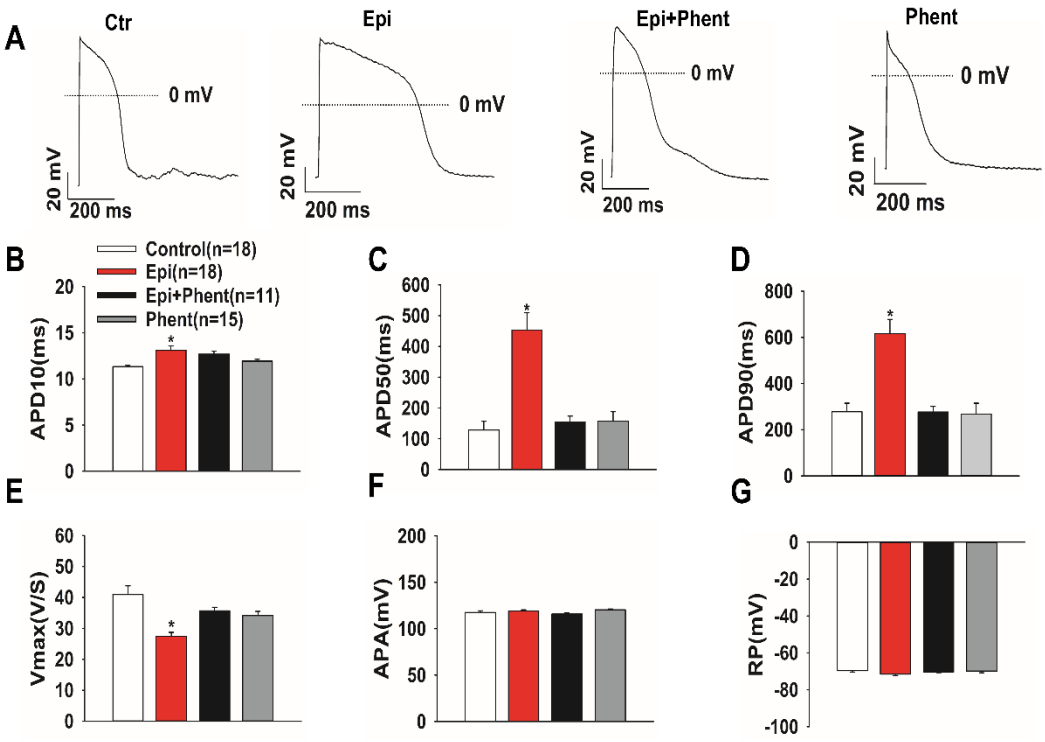

Figure 6. Alpha-adrenoceptor signaling contributed to action potential changes by epinephrine. hiPSC-CMs were treated with either vehicle (Control) or 500 μM phentolamine (Phent) or 500 μM epinephrine (Epi) or epinephrine plus phentolamine (Epi+Phent) for 1 h. Action potentials (AP) were recorded at 1 Hz stimulation. (A) Representative traces of APs in control and epinephrine-treated hiPSC-CMs in the presence and absence of phentolamine. (B) Mean values of APD at 10% repolarization (APD10). (C) Mean values of APD at 50% repolarization (APD50). (D) Mean values of APD at 90% repolarization (APD90). (E) Mean values of maximal upstroke velocity of AP (Vmax). (F) Mean values of action potential amplitude (APA). (G) Mean values of resting potentials (RP). Values given are mean ± SEM. The numbers given in B represent the number of cells for B-G. *p<0.05 versus Control according to one-way ANOVA with Holm-Sidak post-test.

3.5. The α-adrenoceptor activation contributed to occurrence of epinephrine induced arrhythmic events

The changes of APs may cause arrhythmias. Therefore, we tested the possible involvement of the α-adrenoceptor activation in the arrhythmogenesis in setting of catecholamine excess. The same concentration of Epi (500 μM) was applied to spontaneously beating cells. The arrhythmic events including EAD (early afterdepolarization), DAD (delayed afterdepolarization), irregular beating or trigger activity were analyzed. The results showed a significantly increased frequency of the early after-depolarizations (EADs) (red arrow)-like phenomena and delayed after-depolarizations (DADs) (green arrow) -like phenomena and trigger activities (black arrows) in the epinephrine treatment group (Figure 7A and 7B). Interestingly, application of phentolamine (Phent, 500 μM, a non-selective alpha receptor antagonist) suppressed the effect of Epi (Figure 7C).

Statistical analysis showed that only 42% of the cells (6/14) in the control group showed arrhythmic events, whereas 100% of the cells (12/12) in the presence of epinephrine developed arrhythmia (Figure 7D). In the presence of phentolamine, there were still 85% of the cells (6/7) showing arrhythmias but the arrhythmic events were largely reduced (Figure 7D and F, Table 4). The Epi treatment slightly reduced the cells beating rate compared with control group, but it was not statistically significant (Figure 7E, Table 4). These data indicate that high concentration of catecholamines in cardiomyocytes could induce arrhythmias through signaling containing α-adrenoceptor activation.

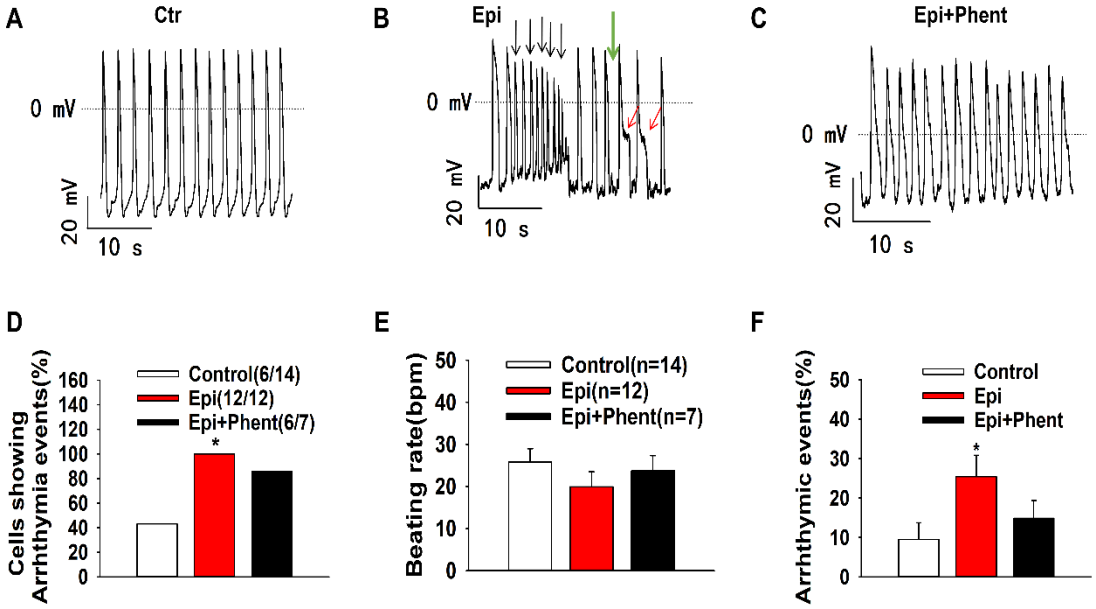

Figure 7. Alpha receptor blocker attenuated arrhythmic events induced by epinephrine. hiPSC-CMs were treated with either vehicle (Control) or 500 μM epinephrine (Epi) or epinephrine plus phentolamine (500 μM, Epi+Phent) for 1 h. Spontaneous action potentials were recorded in spontaneously beating hiPSC-CMs. The occurrence of arrhythmic events (irregular or triggered beats or EAD- or DAD-like events) was compared among the three cell groups. (A) Action potential traces obtained in a cell in the absence of epinephrine. (B) Action potential traces obtained in the presence of epinephrine (Epi) showing EADs (red arrows) and DADs (green arrows) and trigger activities (black arrows). (C) Action potential traces obtained in the presence of phentolamine and epinephrine (Phent+Epi). (D) Summary bar graph showing the effects of Epi and Phent regarding the number of cells showing arrhythmic events (%). (E) Summary bar graph showing the effects of Epi and Phent on the beating rate expressed in beats min^{-1} (bpm). (F) Summary bar graph showing the effects of Epi and Phent on the arrhythmic events (%). The numbers given in D represent the number of cells showing arrhythmic events versus measured total

number of cells. The numbers given in E represent the number of cells for E-F. *p<0.05 versus Control according to the Fisher-test (D) or one-way ANOVA with Holm-Sidak post-test (F).

Table 4. Data from recordings of spontaneous action potentials of hiPSC-CMs.

Group	Control	Epi	Epi+Phent	*p* value
Cell Number	14	12	7	
Number of Cells showing Arrhythmia	6	12	6	
Beating Rate (bpm）	25.79±3.22	19.92±3.58	23.71±3.64	>0.05
Arrhythmic Events (%)	9.5%±4.26%	25.42%±5.41%	14.86%±4.51%	⩽0.01
Sinus rhythm Counts	209	277	199	
Arrhythmia Counts	28	81	26	

Epi: epinephrine; Phent: Phentolamine

3.6. The α1-adrenoceptor activation contributed to effects of epinephrine on APs

Because epinephrine can activate both α1- and α2-receptors and phentolamine is a non-selective α-receptor antagonist, we further used the α1-receptor selective agonists (phenylephrine ,100 μM, 1 h) and α2-receptor selective agonists (clonidine ,10 μM, 1 h), respectively, to clarify which alpha-adrenergic receptor mediated the Epi-effects on APs. Phenylephrine treatment did not change the RP (resting potential) and APA (amplitude of action potential), but reduced Vmax (maximal upstroke velocity) and prolonged APD10 (repolarization at 10%), APD50 (repolarization at 50%) and APD90

(repolarization at 90%) significantly (Figure 8), similar to effects of Epi. After treatment with prazosin (Prazo,1 μM, a selective α1-receptor antagonist) in the presence of phenylephrine, the effect was reversed (Figure 8 B-E). In contrast, clonidine treatment showed no significant effect on AP characteristics of hiPSC-CMs (Figure 8). These data demonstrated that α1-adrenoceptor signaling contributed to the Epi-effects.

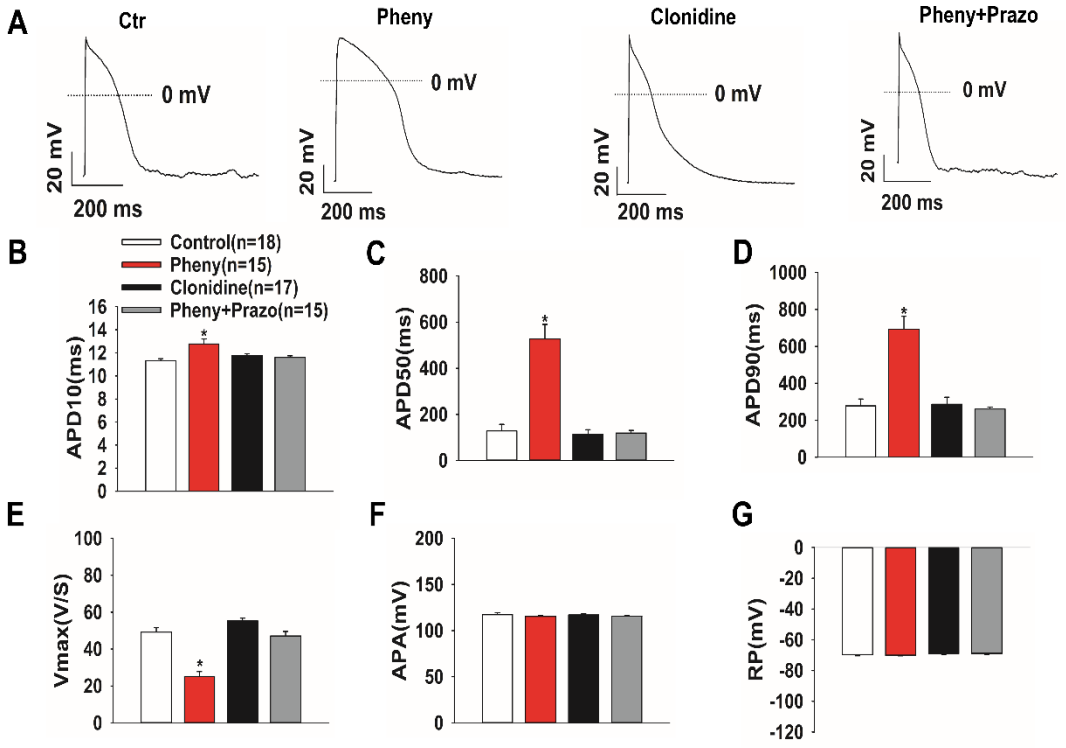

Figure 8. Effects of different alpha-adrenergic receptor agonists on action potentials of hiPSC-CMs. hiPSC-CMs were treated with vehicle (Control) or 100 μM phenylephrine (Pheny) or 100 μM clonidine or phenylephrine plus 100 μM prazosin (Pheny+Prazo) for 1 hour. APs were recorded with 1 Hz stimulation. (A) Representative traces of action potentials (AP) in hiPSC-CMs. (B) Mean values of APD at 10% repolarization (APD10). (C) Mean values of APD at 50% repolarization

(APD50). (D) Mean values of APD at 90% repolarization (APD90). (E) Mean values of maximal upstroke velocity of AP (Vmax). (F) Mean values of action potential amplitude (APA). (G) Mean values of resting potentials (RP). Values given are mean ± SEM. The numbers given in B represent the number of cells for B-G. *p<0.05 versus Control according to one-way ANOVA with Holm-Sidak post-test.

3.7. ROS mediated the effects of the α-adrenoceptor activation

Our previous study detected that beta-adrenoceptor activation contributed to the ROS (oxygen species) production in the presence of high concentration of isoprenaline [57], which led us to test our hypothesis that ROS may also mediate the effects of α-adrenoceptor activation in catecholamine excess. First, we checked the effects of a ROS blocker N-Acetyl-L-cysteine (NAC, 1 mM) on APs in presence of epinephrine or phenylephrine. Indeed, NAC attenuated and H_2O_2 (100 μM, the main form of endogenous ROS) mimicked the Epi- and Pheny-effects on APDs (Figure 9), suggesting involvement of ROS in effects of alpha-adrenoceptor activation. NAC alone showed no effect on APs.

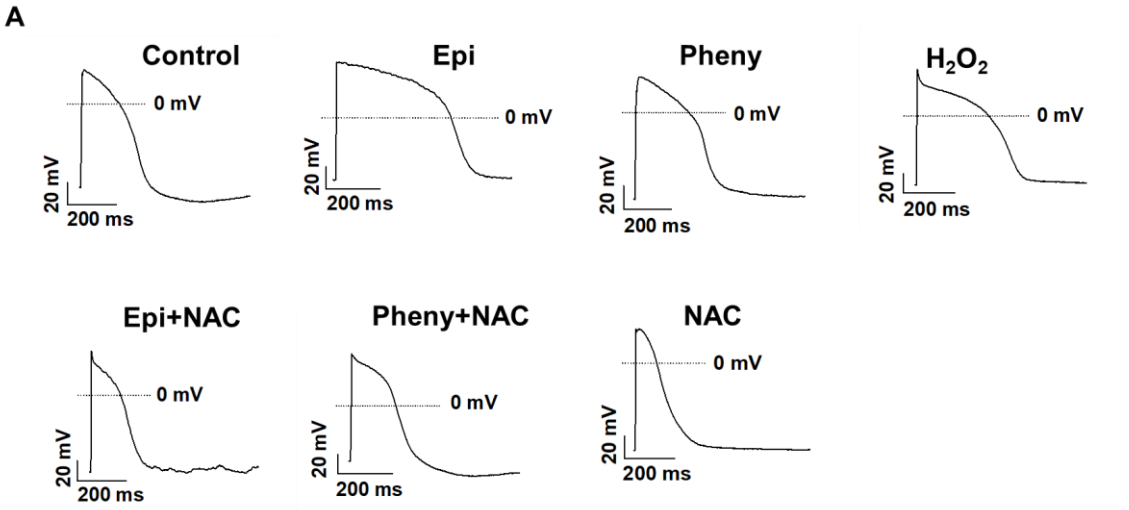

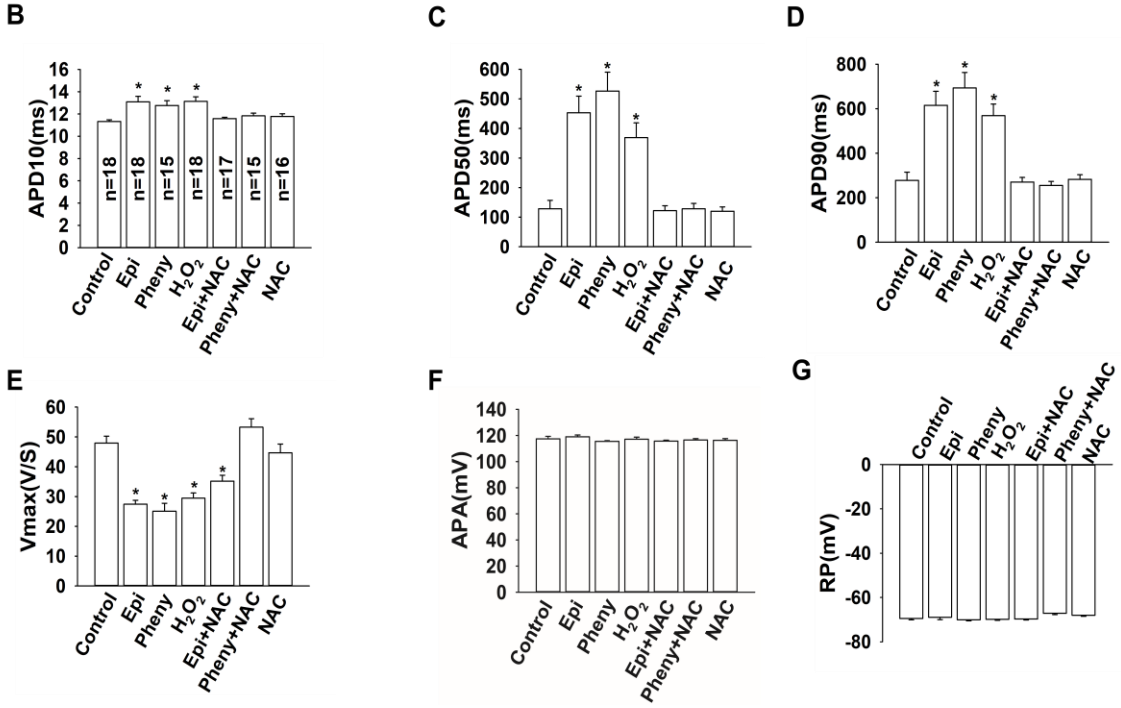

Figure 9. ROS mediated the effects of epinephrine on action potentials. hiPSC-CMs were treated with either vehicle (Control) or 500 μM epinephrine (Epi) or 100 μM phenylephrine (Pheny) or epinephrine plus 1 mM NAC, a ROS-blocker (Epi+NAC,) or phenylephrine plus NAC (Pheny+NAC) or 100 μM H_2O_2 (H_2O_2) or NAC alone for 1 h. Action potentials paced at 1 Hz were recorded. (A) Representative AP-traces of a cell from each group. (B) Averaged values of APD10. (C) Averaged values of APD50. (D) Averaged values of APD90. (E) Averaged values of Vmax. (F) Averaged values of APA. (G) Averaged values of resting potential (RP). The numbers given in B represent the number of cells for B-G. *p<0.05 versus Control according to one-way ANOVA with Holm-Sidak post-test.

Then the ROS-production was assessed by FACS in cells with Epi and Epi plus phentolamine. The ROS-level was increased in Epi-treated cells (Figure 10 C-E, H), suggesting that Epi may affect APs through ROS. Strikingly, the α-adrenoceptor blocker reduced the Epi-induced ROS production in cells (Figure 10 C-F, H), which are indicative of a contribution of α-adrenoceptor

activation to ROS production induced by catecholamine excess. H_2O_2 was used as a positive control for ROS measurements (Figure 10 G, H).

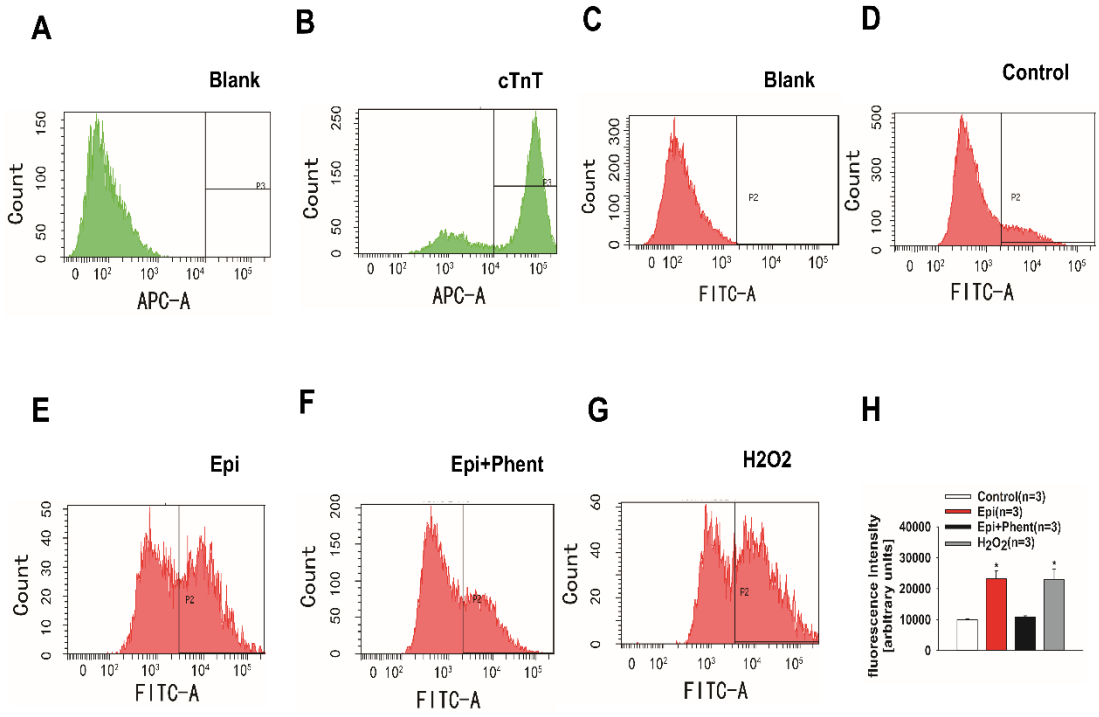

Figure 10. Alpha blocker reduced ROS-production induced by epinephrine. hiPSC-CMs were treated with either vehicle (Control) or 500 µM epinephrine (Epi) or epinephrine plus 500 µM phentolamine (Epi+Phent) for 1 h. ROS-production was measured by FACS and quantified by measuring dichlorofluorescein fluorescence intensity with BD FACS Diva software (Version 8.0.1). (A) and (B) Representative FACS analyses of cTnT: cardiac muscle troponin T (a cardiomyocyte marker) expression in hiPSC-CMs. (C) and (D) Representative FACS analyses of ROS generation in control group. (E) Representative FACS analyses of ROS generation in the presence of epinephrine (Epi). (F) Representative FACS analyses of ROS generation in the presence of epinephrine (Epi) with phentolamine. (G)

Representative FACS analyses of ROS generation in the presence of H_2O_2 (100 μM). (H) Summary of ROS generation from samples in D, E, F and G. “blank” represents control measurements in cells without treatment of the ROS fluorescence dye. Values given are mean ± SEM. “n” represents experimental numbers (biological replicates). *p<0.05 versus Control according to one-way ANOVA with Holm-Sidak post-test.

3.8. NADPH oxidases were involved in effects of α1-adrenoceptor activation

Since ROS production is related to numerus intracellular signaling, we tried to identify a signaling factor responsible for the elevated ROS induced by activation of α1-adrenoceptors. Previous studies have demonstrated that in cardiovascular diseases, the production of reactive oxygen species (ROS) is related to the activation of NADPH oxidase [58]. Therefore, we used diphenyleneiodonium (DPI,10 μM), an inhibitor of NADPH oxidases, to treat cells in the presence of phenylephrine. We observed that the DPI exhibited significant inhibition on the effects of phenylephrine on APs. These data indicate that NADPH oxidases are involved in the activation of α1-adrenoceptor (Figure 11).

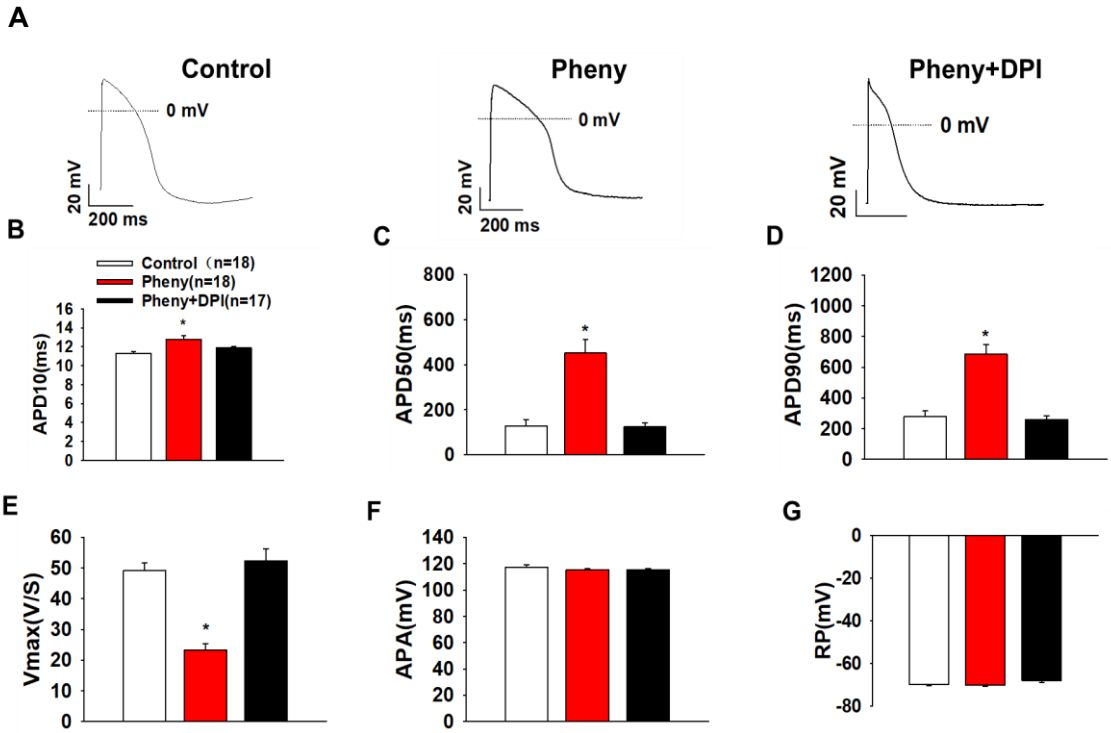

Figure 11. NADPH oxidases were involved in alpha 1-adrenoceptor activation. hiPSC-CMs were treated for 1 h with either vehicle (Control) or 100 μM phenylephrine (Pheny) or phenylephrine plus NADPH inhibitor 10 μM DPI (Pheny+DPI). Action potentials paced at 1 Hz were recorded. (A) Representative traces in a cell from each group. (B) Averaged values of APD10 from each group. (C) Averaged values of APD50 from each group. (D) Averaged values of APD90 from each group. (E) Averaged values of Vmax from each group. (F) Averaged values of APA from each group. (G) Averaged values of resting potential (RP) from each group. The numbers given in B represent the number of cells for B-G. *$p<0.05$ versus Control according to one-way ANOVA with Holm-Sidak post-test.

3.9. Protein kinase C (PKC) was involved in the effects of α1-adrenoceptor activation

Catecholamine mediated generation of ROS can result from the actions of a PLC effector pathway of Gq–coupled GPCR (G-protein coupled receptor)

through PKC [59]. Hence, we examined the possible role of PKC for AP-changes. A PKC-inhibitor (chelerythrine, 10μM) suppressed not only the effects of Epi but also the effects of phenylephrine on APs (Figure 12 A-D). In addition, a PKC stimulator phorbol-12-myristate-13-acetate (PMA) exerted effects on APs similar to that of Epi and Pheny (Figure 12 A, B, D), implying that PKC is required for the effect of α-adrenoceptor activation.

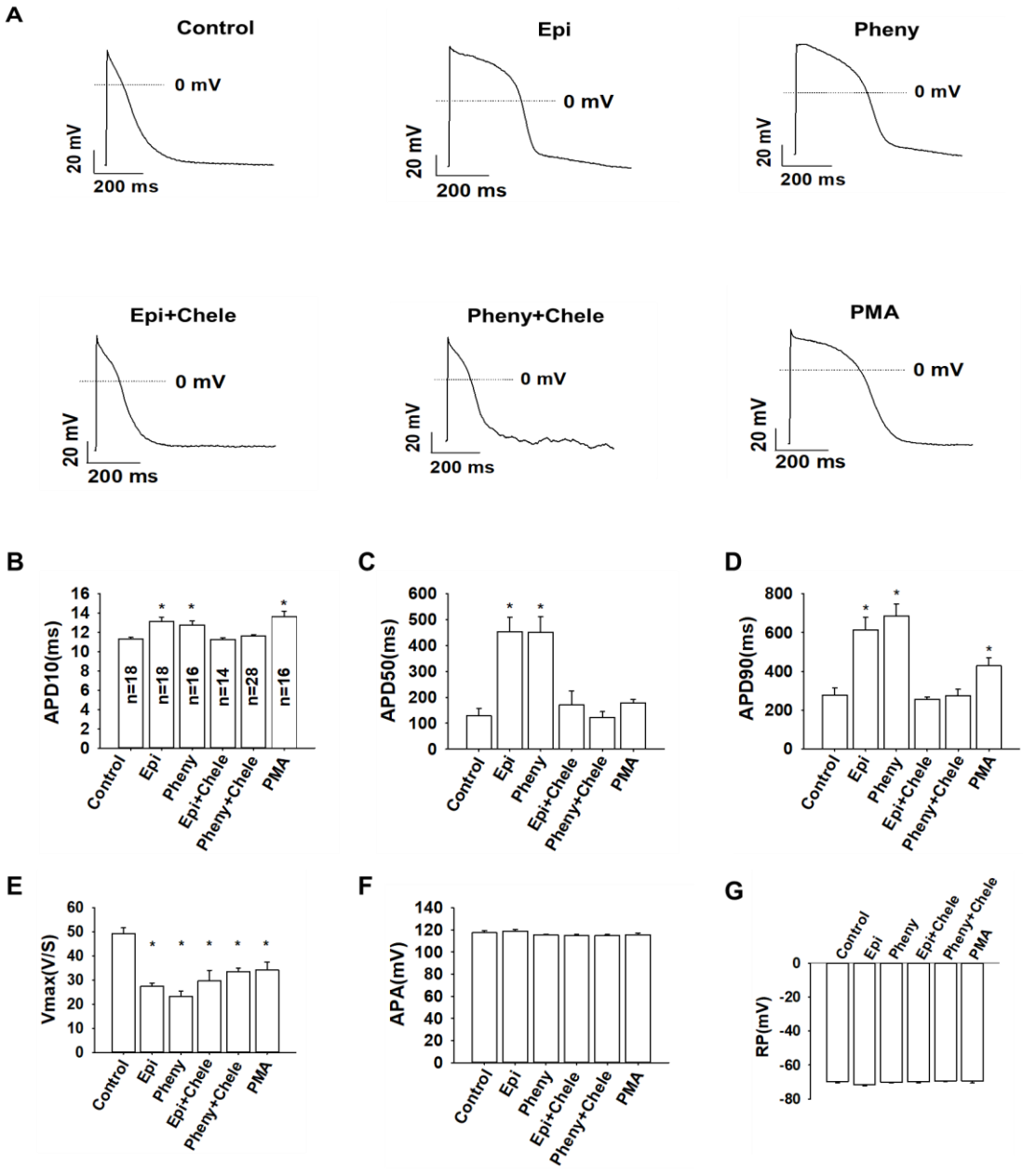

Figure 12. Protein kinase C was involved in alpha 1-adrenoceptor signaling. hiPSC-CMs were treated for 1 h with either vehicle (Control) or 500 μM epinephrine

(Epi) or 100 μM phenylephrine (Pheny), and the epinephrine plus 10μM chelerythrine, an inhibitor of protein kinase C (Epi+Chele) or phenylephrine plus chelerythrine (Pheny+Chele) or 10 μM phorbol-12-myristate-13-acetate (PMA). Action potentials paced at 1 Hz were recorded. (A) Representative traces in a cell from each group. (B) Averaged values of APD10 from each group. (C) Averaged values of APD50 from each group. (D) Averaged values of APD90 from each group. (E) Averaged values of Vmax from each group. (F) Averaged values of APA from each group. (G) Averaged values of resting potential (RP) from each group. The numbers given in B represent the number of cells for B-G. *$p<0.05$ versus Control according to one-way ANOVA with Holm-Sidak post-test.

3.10. Protein kinase C acted as a downstream factor of ROS

Given that both ROS and PKC were involved in α1-adrenoceptor activation, we intended to reveal whether PKC is a downstream or upstream signaling of ROS in α-adrenoceptor activation. Cells were challenged by H_2O_2 in presence and absence of the PKC-inhibitor (chelerythrine). The PKC-inhibitor did suppress the effects of H_2O_2 (Figure 13), suggesting that PKC acted as a downstream signaling factor of ROS in the signal pathway.

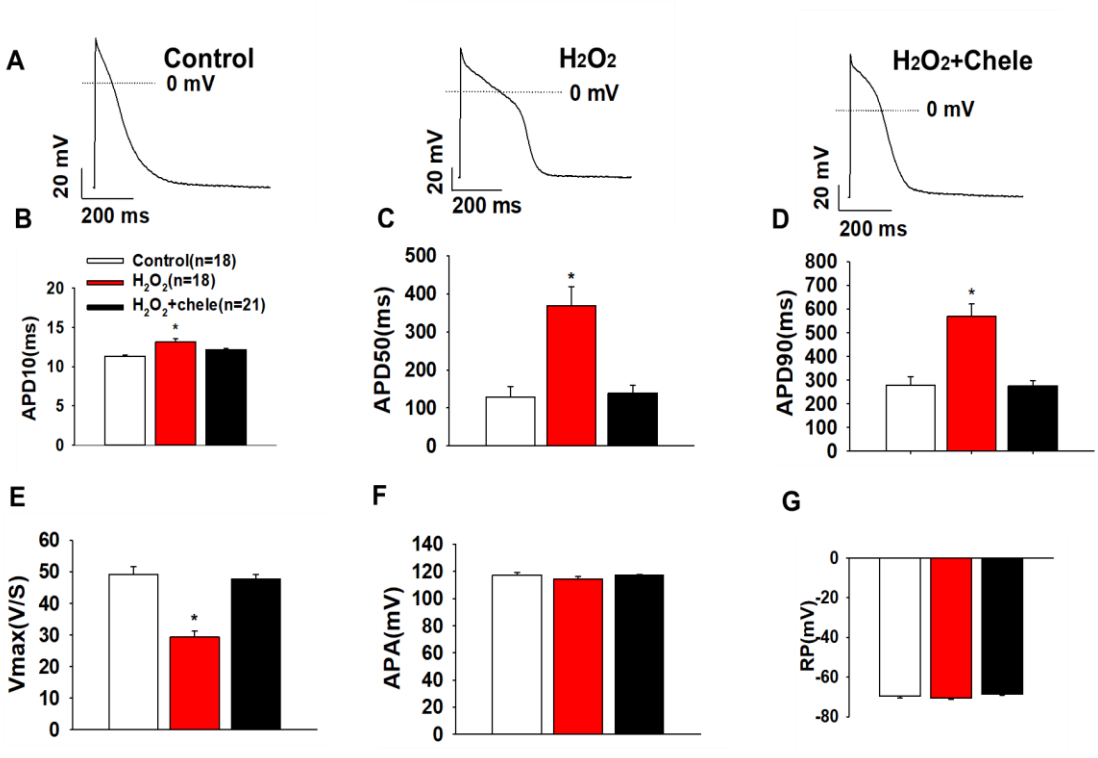

Figure 13. Protein kinase C was a downstream factor of ROS. hiPSC-CMs were treated for 1 h with either vehicle (Control) or 100 μM H_2O_2 (H_2O_2) or H_2O_2 plus 10 μM chelerythrine (H_2O_2+Chele). Action potentials paced at 1 Hz were recorded. (A) Representative traces in a cell from each group. (B) Averaged values of APD10 from each group. (C) Averaged values of APD50 from each group. (D) Averaged values of APD90 from each group. (E) Averaged values of Vmax from each group. (F) Averaged values of APA from each group. (G) Averaged values of resting potential (RP) from each group. The numbers given in B represent the number of cells for B-G. *p<0.05 versus Control according to one-way ANOVA with Holm-Sidak post-test.

3.11. The ionic mechanisms of AP-changes induced by α-adrenoceptor activation

To investigate the underlying ionic currents responsible for aforementioned APD changes, we evaluated the effects of epinephrine (Epi) or phenylephrine (Pheny) on different ion channel currents. First, the effects of Epi or Pheny on inward currents I_{Na}, I_{CaL}, and I_{NCX} were checked in vehicle- (control) or Epi- or Pheny-treated cells. The peak I_{Na} (I_{Na-p}) was reduced by Epi (Figure 14 A, C, G). The late I_{Na} (I_{Na-L}), however, was slightly increased by Epi (Figure 14 B). Phentolamine (Phent) prevented the Epi effect on I_{Na-p}, suggesting α-adrenoceptor activation may contribute to the inhibitory effect. Pheny was applied to stimulate α1-adrenoceptor. Indeed, Pheny mimicked Epi effect on I_{Na-p} (Figure 14 A, C, G), which confirmed the contribution of α1-adrenoceptor signaling to the inhibition of I_{Na-p}. Further, the sodium channel kinetic parameters were analyzed. Epi but not Pheny enhanced the voltage-dependent inactivation of the channel by shifting the inactivation curves (evaluated by the potential of 50% inactivation (V0.5)) to more negative potentials (Figure 14 E, I). Both Epi and Pheny failed to influence the activation and recovery from inactivation (Figure 14 D, H and F, J). Strikingly, the Epi effect on the inactivation was not reversed by the α-adrenoceptor blocker (Figure 14 I).

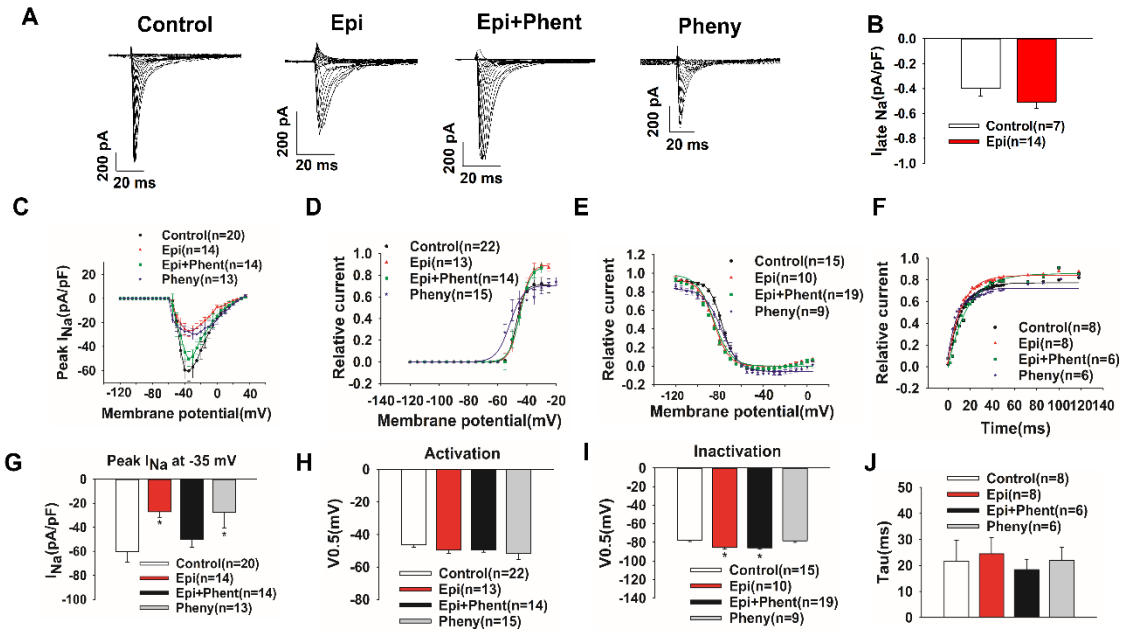

Figure 14. Sodium channel currents was changed by alpha-adrenoceptor activation. hiPSC-CMs were treated for 1 h with vehicle (Control) or 500 μM epinephrine (Epi) or epinephrine plus 500 μM phentolamine (Epi+Phent) or 100 μM phenylephrine (Pheny). (A) Representative traces of sodium channel currents (I_{Na}). (B) Mean values of late I_{Na} in absence and presence of epinephrine (Epi). (C) I-V curves of $I_{Na\text{-}p}$ from each group. (D) Activation curves of $I_{Na\text{-}p}$ from each group. (E) Inactivation curves of $I_{Na\text{-}p}$ from each group. (F) Time course curves of recovery from inactivation. (G) Mean values of $I_{Na\text{-}p}$ at -35 mV. (H) Mean values of potentials at 50% activation (V0.5). (I) Mean values of potentials at 50% inactivation (V0.5). (J) Mean values of time constants (Tau) of recovery from inactivation. “n” represents number of cells. *p<0.05 versus Control according to the analysis of one-way ANOVA with Holm-Sidak post-test.

The L-type calcium channel current ($I_{Ca\text{-}L}$) was significantly enhanced by Epi (Figure 15 A-B, F). The α-adrenoceptor blocker (Phent) blocked and the α1-adrenoceptor agonist (Pheny) mimicked the Epi effect (Figure 15 A-B, F),

indicative of roles of α1-adrenoceptor signaling for the enhancement of $I_{Ca\text{-}L}$. However, Epi and Pheny changed the channel kinetics differentially. Epi enhanced the channel activation significantly by shifting the activation (evaluated by the potential of 50% activation (V0.5)) to a more negative potential, without influencing the inactivation of $I_{Ca\text{-}L}$ (Figure 15 C-D, G-H). While Pheny changed the channel activation only slightly but strongly enhanced the inactivation by shifting the inactivation curve to a more negative potential (Figure 15 C-D, G-H). Both Epi and Pheny failed to influence the time course of recovery from inactivation (Figure 15 E, I).

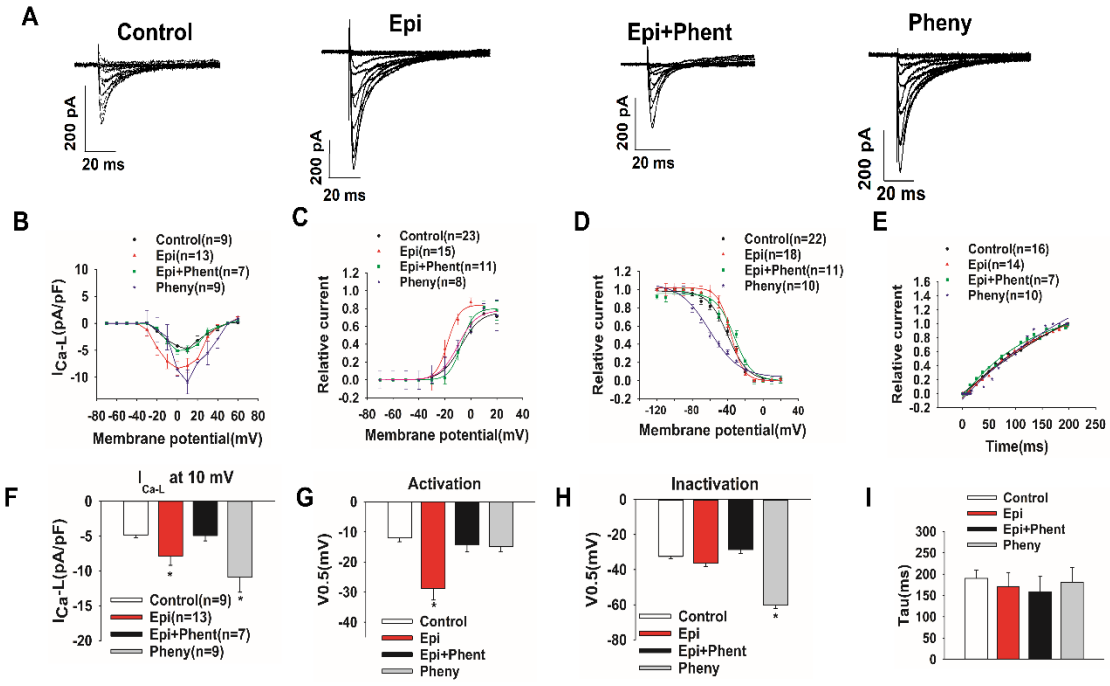

Figure 15. L-type calcium channel currents was changed by alpha-adrenoceptor activation. hiPSC-CMs were treated for 1 h with vehicle (Control) or 500 μM epinephrine (Epi) or epinephrine plus 500 μM phentolamine (Epi+Phent) or 100 μM phenylephrine (Pheny). (A) Representative traces of L-type calcium channel currents

($I_{Ca\text{-}L}$). (B) I-V curves of $I_{Ca\text{-}L}$ from each group. (C) Activation curves of $I_{Ca\text{-}L}$ from each group. (D) Inactivation curves of $I_{Ca\text{-}L}$ from each group. (E) Time course curves of recovery from inactivation. (F) Mean values of $I_{Ca\text{-}L}$ at 10 mV. (G) Mean values of potentials at 50% activation (V0.5). (H) Mean values of potentials at 50% inactivation (V0.5). (I) Mean values of time constants (Tau) of recovery from inactivation. The numbers given in B-E represent the number of cells also for F-I, respectively. *p<0.05 versus Control according to one-way ANOVA with Holm-Sidak post-test.

The Na^+/Ca^{2+} exchanger current (I_{NCX}) can also influence APD. So, we checked whether it participated in the APD-prolongation induced by Epi. In hiPSC-CMs treated by Epi, I_{NCX} was only slightly enhanced, which did not reach the statistical significance (Figure 16).

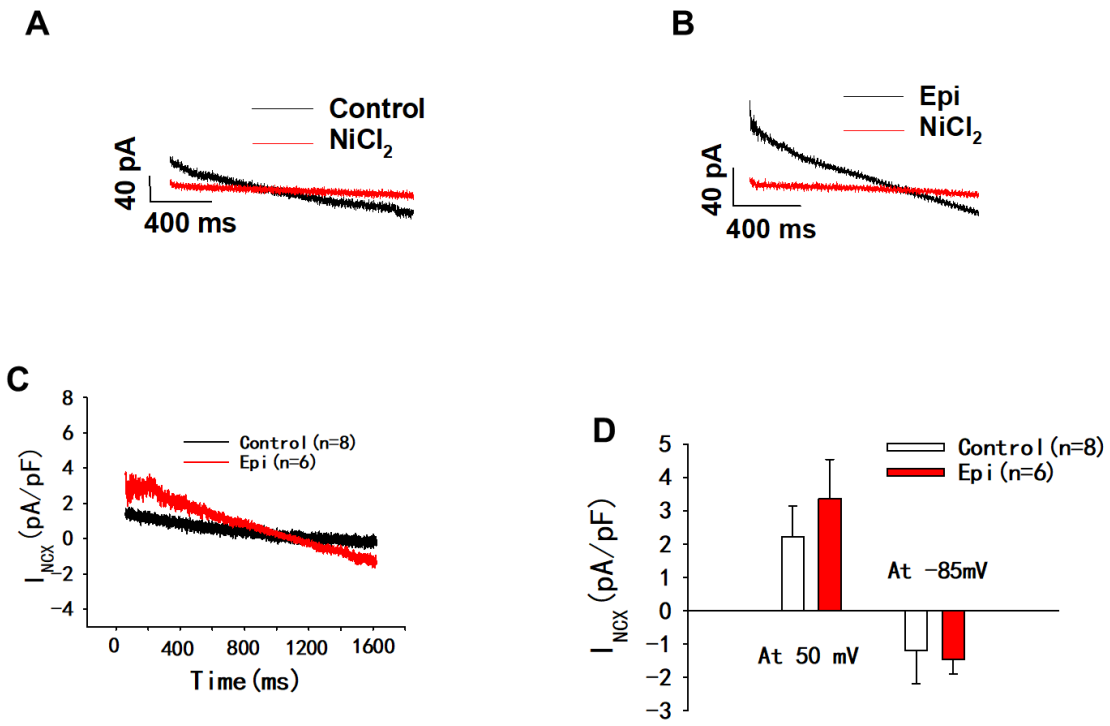

Figure 16. Na^+/Ca^{2+} exchanger currents in the presence of epinephrine. hiPSC-CMs were treated for 1 h with vehicle (Control) or 500 μM epinephrine. $NiCl_2$ (3 mM), an inhibitor of Na^+/Ca^{2+} exchanger current (I_{NCX}), was used to separate the I_{NCX}

from other currents. (A-B) Representative current traces in hiPSC-CMs treated with vehicle (Control) or epinephrine (Epi) in the absence (black line) and presence of $NiCl_2$ (red line). (C) Representative traces of $NiCl_2$-sensitive currents (I_{NCX}) in hiPSC-CMs treated with vehicle (Control) or epinephrine (Epi). (D) Mean values of I_{NCX} at 50 mV and -85 mV in absence (Control) and presence (Epi) of epinephrine. “n” represents number of cells.

Next, we evaluated the outward K^+ currents including the transient outward K^+ currents (I_{to}) and rapidly activating delayed rectifier current (I_{Kr}). Epi showed no significant effect on I_{to} (Figure 17). I_{Kr} was slightly attenuated by Epi, but largely suppressed by Pheny (Figure 18). Pheny failed to change the channel activation (Figure 18 D-E), inconsistent with reduced I_{Kr} in the presence of Pheny.

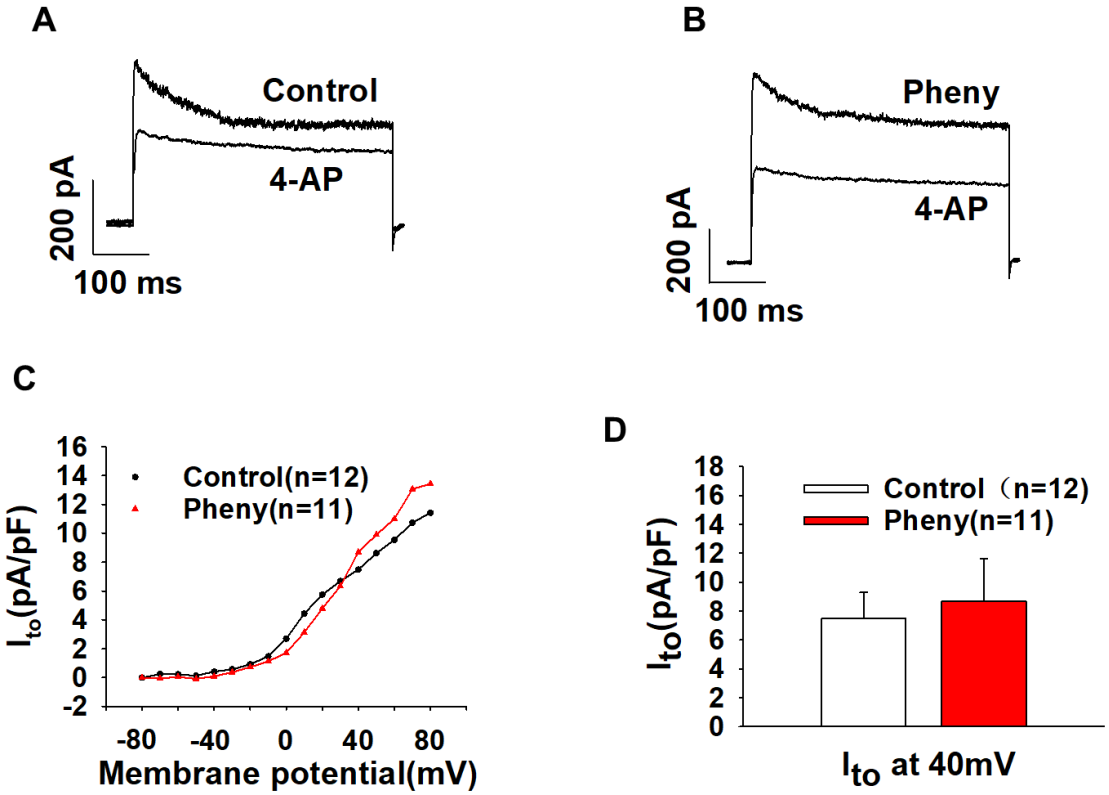

Figure 17. Transient outward currents (I_{to}) in the presence of phenylephrine. hiPSC-CMs were treated for 1 h with vehicle (Control) or 100 μM phenylephrine (Pheny). 4-AP (3 mM), an inhibitor of I_{to}, was used to separate I_{to} from other currents. (A-B) Representative current traces in hiPSC-CMs treated with vehicle (Control) or phenylephrine (Pheny) in the absence and presence of 4-AP. (C) I-V curves of 4-AP-sensitive currents (I_{to}) in hiPSC-CMs treated with vehicle (Control) or phenylephrine (Pheny). (D) Mean values of I_{to} at 40 mV in absence (Control) and presence (Pheny) of phenylephrine. "n" represents number of cells.

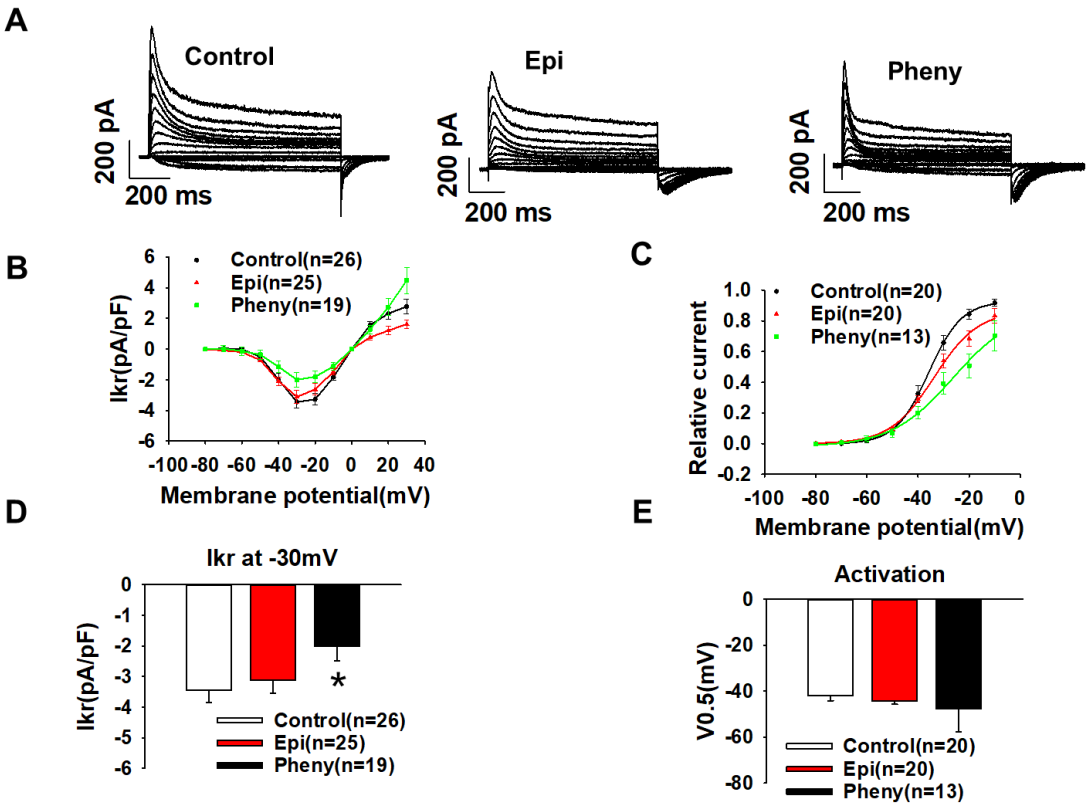

Figure 18. Rapidly activating delayed rectifier K channel currents (I_{Kr}) in the presence of epinephrine and phenylephrine. hiPSC-CMs were treated for 1 h with vehicle (Control) or 500 μM epinephrine or 100 μM phenylephrine. Cs^+ instead of K^+ was used as the charge carrier to record the Cs^+ currents conducted by HERG channels (I_{Kr}). (A) Representative current traces of I_{Kr} in hiPSC-CMs treated with

vehicle (Control) or epinephrine (Epi) or phenylephrine (Pheny). (B) I-V curves of I_{Kr} in each group. (C) Activation curves of I_{Kr} in each group. (D) Mean values of I_{Kr} at -30 mV in each group. (E) The potentials at 50 % activation (V0.5) of I_{Kr} in each group. “n” represents number of cells. *p<0.05 versus Control.

3.12. The hiPSC-CMs from a second (D2) and third (D3) donor recapitulated some key results in cells from the first donor (D1)

Considering that all the experiments described above were performed in hiPSC-CMs from one healthy donor (D1), some important experiments were repeated in hiPSC-CMs from another two subjects (D2 and D3). The results showed that in both D2 (Figure 19) and D3 (Figure 20) hiPSC-CMs, the alpha 1-adrenoceptor activator phenylephrine changed AP parameters in the same manner as in D1 cells. Also, as in D1 cells, the alpha 2-adrenoceptor agonist clonidine did not influence APs. Both the positive (significant effects) and negative (no effects) results obtained in D1-hiPSC-CMs were successfully reproduced in D2- and D3-hiPSC-CMs, implying that the individual variation is not large.

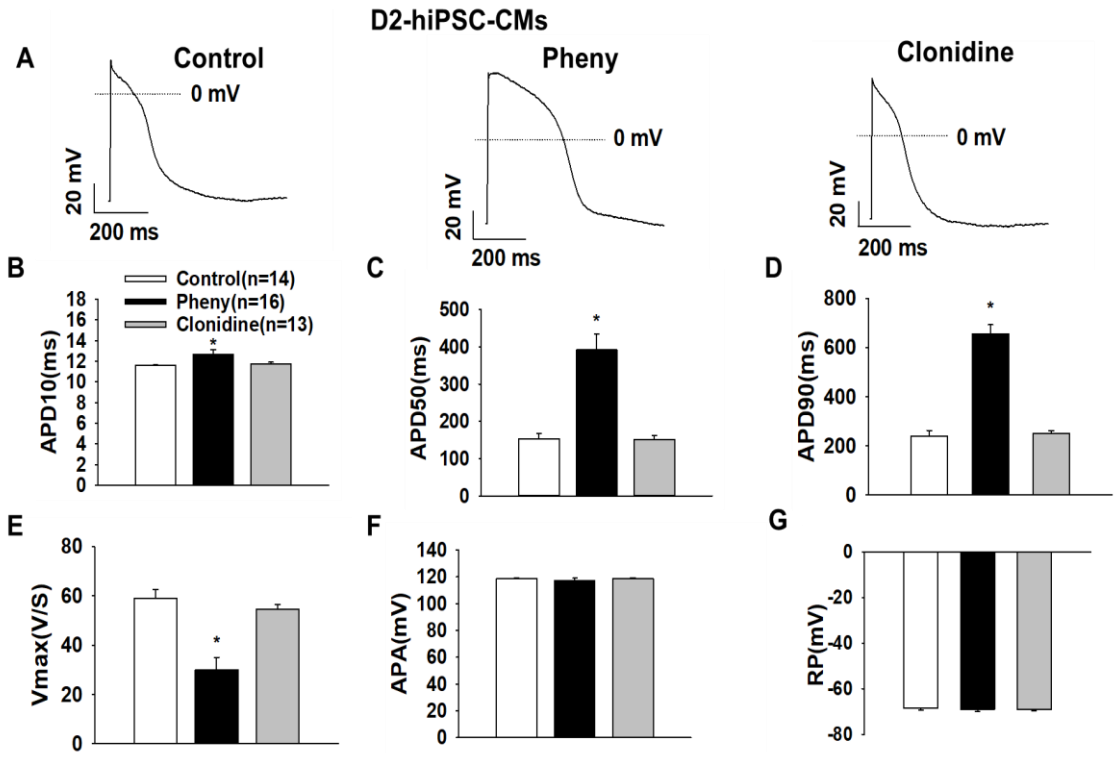

Figure 19. hiPSC-CMs from the second donor mimicked results obtained in hiPSC-CMs from the first donor. A second donor (D2) was recruited and hiPSC-CMs were generated (D2-hiPSC-CMs). Experiments were carried out under the same conditions as that in D1 cells. The cells were treated with either vehicle (Control) or 100 μM phenylephrine (Pheny) or 100 μM clonidine. (A) Representative AP-traces of a cell from each group. (B) Averaged values of APD10. (C) Averaged values of APD50. (D) Averaged values of APD90. (E) Averaged values of Vmax. (F) Averaged values of APA. (G) Averaged values of resting potential (RP). The numbers given in B represent the number of cells for B-G. *$p<0.05$ versus Control according to one-way ANOVA with Holm-Sidak post-test.

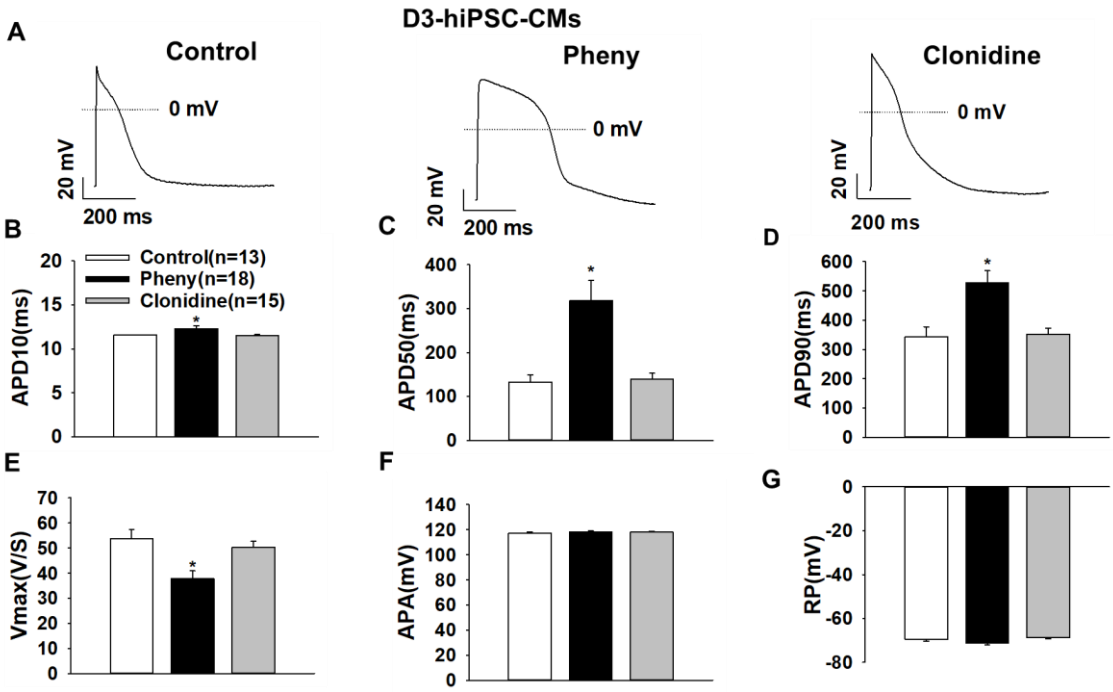

Figure 20. hiPSC-CMs from the third donor mimicked results obtained in hiPSC-CMs from the first donor. A third (D3) donor was recruited and hiPSC-CMs were generated (D3-hiPSC-CMs). Experiments were carried out under the same conditions as that in D1 cells. The cells were treated with either vehicle (Control) or 100 μM phenylephrine (Pheny) or 100 μM clonidine. (A) Representative AP-traces of a cell from each group. (B) Averaged values of APD10. (C) Averaged values of APD50. (D) Averaged values of APD90. (E) Averaged values of Vmax. (F) Averaged values of APA. (G) Averaged values of resting potential (RP). The numbers given in B represent the number of cells for B-G. *$p<0.05$ versus Control according to one-way ANOVA with Holm-Sidak post-test.

4. DISCUSSION

4.1. Main findings and the importance of the study

To our knowledge, this is the first study using hiPSC-CMs to investigate the roles and mechanisms of alpha 1-adrenoceptor signaling for the ion channel dysfunction, APD-prolongation and occurrence of arrhythmias caused by toxic effects of high concentration of catecholamine. The novel findings in this study include (i) high concentration of epinephrine can prolong APD through activating alpha 1-adrenoceptors in hiPSC-CMs; (ii) high concentration epinephrine can trigger arrhythmias through activating alpha 1-adrenoceptors in hiPSC-CMs; (iii) ROS signaling contributes to APD-prolongation induced by activating alpha 1- adrenoceptors in hiPSC-CMs; (iv) NADPH oxidases are involved in effects of alpha 1-adrenoceptor activation in hiPSC-CMs; (v) PKC acts as a downstream factor of ROS in alpha 1-adrenoceptor activation; (vi) Na, L-type Ca and HERG channel dysfunctions contribute to AP-changes caused by alpha 1-adrenoceptor activation in hiPSC-CMs.

Takotsubo cardiomyopathy is a unique acute cardiac attack and occurs predominantly in postmenopausal women in association with emotional or physical stress or administration of catecholamines such as epinephrine [22, 60, 61]. Although the pathological changes in heart of TTC-patients are generally reversible when appropriate treatment is carried out, the in-hospital mortality rate of TTC is similar to that of acute coronary syndromes [11]. The primary manifestation may occur with different complications containing ventricular tachyarrhythmias. According to reported data, the prevalence of arrhythmias such as ventricular tachycardia, ventricular fibrillation and atrioventricular nodal block can reach 14% of TTC-cases, mainly in the setting of long QTc [62]. When TTC-patients suffered from arrhythmias, the long-term mortality was elevated [63]. It is well documented that TTC is related to QT

prolongation [64], so exploring the pathogenic mechanisms of QT prolongation in the setting of TTC is clinically relevant.

So far it has been well established that catecholamine excess may play a central role in the pathogenesis of TTC. The beta-adrenoceptor, especially beta1-receptor, is the most important adrenoceptor in cardiomyocytes and most studies on the pathogenesis of TTC focused on beta-adrenoceptor signaling. However, some clinical studies showed that some TTC-patients did not profit from beta-blocker treatment. Furthermore, animal studies demonstrated that combination of alpha-blocker and beta-blocker improved the efficacy of treatments against TTC-phenotypic changes. Taken all together, alpha-adrenoceptor activation in the setting of TTC may play an important role for pathogenesis of TTC, but studies on roles of alpha-adrenoceptor signaling for TTC remain spars. The study on roles of alpha-adrenoceptor signaling for long QTc and arrhythmogenesis in TTC is still lacking. This study revealed that high concentration of catecholamine can enhance $I_{Ca\text{-}L}$ and reduced I_{Kr} via alpha1-receptor signaling, leading to APD-prolongation (equivalent to QT-prolongation in patients) and arrhythmic events. The study provided ionic and molecular mechanisms for understanding the occurrence of long QTc and arrhythmias in the setting of TTC or other cardiac disorders related with toxic catecholamine effects. Furthermore, this study may also provide novel information for the therapy of TTC or other heart diseases associated with catecholamine excess.

4.2. Possible mechanisms underlying AP-changes and arrhythmias induced by toxic catecholamine via alpha-adrenoceptor activation

The fact that TTC is usually triggered by stress, under which sympathetic activity is enhanced and catecholamine release is elevated [65], suggests roles of catecholamine excess for the incidence of arrhythmias or heart failure. However, the underlying mechanisms still need to be clarified. The regional

wall-motion abnormality in left ventricle, the important clinical feature of TTC, provided a hint for studies. It has been shown that the sympathetic innervation in the basal myocardium is higher than that in the apex. On the contrary, the ß-adrenoceptor (ß-AR) density is higher in apical than in basal myocytes [66]. Thus, the apical cells may response to catecholamine more strongly than basal myocytes. Indeed, several studies showed that isoprenaline exerts stronger effect on apical than basal cardiomyocytes in the left ventricle [67-69]. These data indicate that the high ß-AR density plays a critical role for the regional cardiac dysfunction and happening of TTC.

Here, another question to be addressed is how catecholamine exerts a negative inotropic effect. It has been shown that ß2-AR can couple to G_s-adenylate cyclase-cAMP or G_i or non-G-protein pathways [70, 71]. When catecholamine concentration is high, ß2-AR mainly couples to G_i protein, which can suppress the cardiac contraction through reducing intracellular cAMP level [27, 72]. Thus, the negative inotropic effect in apical myocytes is relatively larger than that in basal myocytes, leading to increased outflow resistance of the ventricular blood and resulting in a ballooning change of ventricle. Whether arrhythmias in TTC are also associated with the regional difference of sympathetic nerve innervations and adrenoceptor distributions is still unknown. Whether the α-adrenoceptor mediated signaling plays an important role for APD-prolongation and appearance of arrhythmias in TTC is so far unclear.

In the present study, to test our hypothesis that α-adrenoceptor signaling may play roles for arrhythmias caused by toxic effects of catecholamine, we investigated the possible contributions of α-adrenoceptor signaling to the acquired LQT and arrhythmogenesis in the setting of TTC (high concentration of catecholamine). We used a high concentration of epinephrine (Epi), which is a native catecholamine in vivo and can be used to stimulate both α-and

β-adrenoceptors, and different α-adrenoceptor blockers or activators for the study. Epi prolonged APD and reduced V_{max} of APs. An α-adrenoceptor blocker, phentolamine (blocking alpha 1-and alpha 2-receptor), reversed the effects of epinephrine, implying that alpha-adrenoceptor signaling contributes to effects of epinephrine. To confirm the involvement and subtype of α-adrenoceptors in the observed effects, more specific agonists and antagonists of α-receptors were applied. Phenylephrine (mainly activates alpha1-receptors) but not clonidine (mainly activates α2-receptors) mimicked the Epi-effects and prazosin (α1-receptor specific blocker) abolished the effects of phenylephrine, indicating that α1-adrenoceptor activation contributed to the changes of APs in presence of high doses of catecholamine.

Ample clinical evidence has demonstrated that excessive prolongation of the action potential duration (APD) may lead to ventricular tachyarrhythmia [73]. The APD-prolongation reflects the QT-prolongation on ECG in patients and is the culprit for occurrence of arrhythmias in long QT-syndrome. In contractile myocytes , APs are triggered by the acute entrance of sodium ions (Na^+) inside the cell, resulting in an inward current (I_{Na}) that shifts the membrane potential from its resting state to a depolarization state [74], which evokes a contraction of the cardiomyocyte through “Excitation-Contraction Coupling”. The maximal velocity (Vmax) of the depolarization is critical for the speed of excitation conduction. The reduction of V_{max} of APs may decelerate electrical pulse propagation and cause conduction defect in the heart. Both changes (the APD-prolongation and suppression of Vmax) detected in the presence of high concentration epinephrine are substrates for occurrences of arrhythmias. Our study, indeed, detected that arrhythmic events were induced by epinephrine and were attenuated by the α-adrenoceptor blocker, indicative of the involvement of α-adrenoceptor signaling in occurrence of arrhythmias in the setting of TTC. In the presence of Epi, more cells showed arrhythmic events. The α-blocker failed to reduce significantly the number of cells

showing arrhythmic events, suggesting that the α-blocker only reduced but did not terminate the arrhythmic events in most cells. Epi slightly slowed cell beating, probably representing a toxic effect of high concentration of catecholamine.

Previous studies have shown that reactive oxygen species (ROS) are not only toxic by-products of aerobic metabolism, but also can be used as intracellular signaling molecules in vascular cells [75]. Excessive production of ROS causes oxidative stress, which relates to many cardiovascular diseases [76]. To further explore the signal factors related to alpha-receptor activation, we checked ROS production. Actually, our data demonstrated that alpha-receptor activation also contributes to the enhancement of ROS production induced by catecholamine. We observed that (1) the α-adrenoceptor blocker reduced Epi induced ROS generation; (2) an antioxidant, N-acetyl-L-cysteine (NAC, a ROS blocker) blocked the effects of Epi and Pheny on APs; (3) Hydrogen peroxide H_2O_2 (a form of endogenous ROS) mimicked Epi and Pheny effects on APs. These data demonstrated an important role of ROS for AP-changes associated with α-adrenoceptor activation.

The next question is how the ROS-level was elevated by α-adrenoceptor activation. To figure it out, we tried to use inhibitors for NADHP oxidases, which are known to be important for ROS generation. Actually, the NADPH oxidase blocker DPI attenuated the effects of Pheny, implying that NADPH oxidases were in the signaling responsible for AP changes evoked by α-adrenoceptor activation. How NADPH oxidases were activated and whether other ROS-linked signaling were involved in α-adrenoceptor activation need to be assessed in further studies.

Previous studies have shown that the α1-adrenoceptor is coupled to phospholipase C and PKC [77, 78]. Then we examined the possible involvement of PKC, another important factor of alpha-receptor signaling, in

the toxic effects of catecholamine. To unveil PKC effects in α-adrenoceptor activation, both PKC blocker and activator were employed. The PKC-blocker (chelerythrine) inhibited the effects of both Epi and Pheny and the PKC activator (PMA) mimicked their effects on APs, which confirmed a role of PKC activation for α-adrenoceptor mediated effects. With respect of the mechanisms underlying PKC activation, the existence of α1-adrenoceptor and Gq in hiPSC-CMs may help us understand it as that the activation of α1-receptor stimulates Gq protein and then stimulates PLC, which initiates its downstream signaling including PKC activation. Although the Gq-PLC-PKC signaling is a well-known and typical pathway for Gq-coupled receptors, we found that PKC is a downstream factor of ROS because the PKC blocker abolished the ROS effect. Given that NADPH oxidases were also involved in effects of α1-receptor activation because its inhibitor (DPI) blocked the effects of phenylephrine, we can interpret the signaling in α1-adrenoceptor activation by high concentration of catecholamine as; α1-adrenoceptor-Gq-PLC-NADPH-ROS-PKC. Here how PLC evokes NADPH oxidase activation is still an open question and further studies are needed to answer it.

Ion-channel dysfunctions are associated with numerus cardiac disorders including Long QT syndrome (LQTS) [79]. The normal rhythm of the heart results from the regular electrical activity based on transmembrane currents conducted by different ion channels in cardiomyocytes [74]. The most important currents are I_{Na}, $I_{Ca\text{-}L}$ and potassium currents. The modification of ion channels may lead to electrical instability and predisposition to ventricular arrhythmias. Therefore, we researched the ionic mechanism underlying the AP-changes induced by alpha-adrenoceptor activation.

To test our another hypothesis that α1-adrenoceptor signaling may contribute to ion channel dysfunctions caused by catecholamine excess, different ion

channel currents were assessed in the presence of high concentration of epinephrine and α-adrenoceptor agonist or antagonist.

The peak I_{Na} was suppressed by epinephrine and reversed by the alpha-receptor blocker. Likewise, the α1-receptor agonist (Pheny) inhibited I_{Na}, hinting at a modulation SCN5A channels by α1-adrenoceptor signaling. The facts that Pheny did change the channel gating kinetics and the α-adrenoceptor blocker failed to reverse the Epi-effect on the channel inactivation suggest that the suppression of I_{Na} did not result from changes of sodium channel gating kinetics. Of note, the influence of epinephrine on SCN5A expression (a reduction) was consistent with its effect on peak I_{Na}. All data together showed that α-adrenoceptor activation changes mainly the channel expression level. The suppression of I_{Na} can explain reduction of Vmax of APs.

The L-type Ca channel currents ($I_{Ca\text{-}L}$) were enhanced by alpha-receptor signaling through enhancing the channel activation, which was confirmed by the evidences that Epi increased $I_{Ca\text{-}L}$ and the α-receptor blocker reduced Epi effects and additionally, Pheny mimicked Epi effects. The expression level of L-type Ca channel (CACNA1C) was also increased, which is in agreement with $I_{Ca\text{-}L}$ enhancement and suggests that alpha-receptor signaling regulated both the channel activity and expression level. The enhancement of $I_{Ca\text{-}L}$ is in agreement with the APD-prolongation.

The hERG (human ether-a-go-go related gene) channel ($K_{v11.1}$) underlying the rapid component of delayed rectifier potassium current (I_{Kr}) is critical for the repolarization of cardiomyocytes and a blockade of hERG channels can produce an excessive prolongation of action potential duration [80]. Moreover, hERG channel is the target of many drugs that exert either therapeutic or side effects in the heart. We observed that toxic doses of catecholamine suppressed the channel expression but not the channel activation, leading to

reduced HERG channel current (I_{Kr}). Reduced I_{Kr} can prolong APD and contribute to occurrence of arrhythmic events. Therefore, the suppression of I_{Kr} by α1-receptor activation may contribute to APD/QT prolongation and arrhythmogenesis of TTC or other cardiac disorders caused by toxic effects of catecholamine.

Some other currents that may contribute to AP morphology including the transient outward current (I_{to}) and Na^+/Ca^{2+} exchanger current (I_{NCX}) were also assessed. Both currents were only slightly enhanced by Epi or Pheny and the enhancement did not reach statistical significance, suggesting the role of I_{to} and I_{NCX} for the arrhythmogenesis in α-adrenoceptor activation is negligible. This is different from β-adrenoceptor activation. In our previous study, we observed that isoprenaline (activating β-receptors rather than α-receptors) significantly suppressed I_{to} [57], suggesting a contribution of I_{to} to APD-prolongation induced by β-receptor activation.

Here a next question is how the Na (SCN5A), L-type Ca (CACNC1C) and HERG (I_{Kr}) channels were regulated by α1-adrenoceptor activation. The mechanisms behind the modulation of these channels may be complex because many factors linked to the signaling of α1-receptor-Gq-PLC-NADPH-ROS-PKC figured out in this study may participate in the modulation of these channels. For example, ROS and PKC are known as important regulators of different ion channels [81-83]. Whether ROS and PKC can directly or indirectly (through other downstream factors) regulate the three types of channels, and more importantly, whether they mediate the suppression of the SCN5A and HERG and the enhancement of L-type Ca channel currents and expression levels when α1-adrenoceptors are activated, need to be investigated by further studies.

Taken together, the study demonstrated that alpha 1-receptor activation induced ion channel dysfunctions, mainly affecting of I_{Na}, $I_{Ca\text{-}L}$ and I_{Kr} by

changing their channel gating or expression in cardiomyocytes. The ion channel dysfunctions led to abnormal APs (reduction of Vmax and prolongation of APD) and hence facilitated occurrence of arrhythmic events, suggesting a possible responsibility of alpha 1-receptor signaling for occurrence of arrhythmias in high concentration of catecholamine. The toxic effects of catecholamine excess contained the effects of the α1-adrenoceptor mediated signaling, α1-Gq-PLC-NADPH-ROS-PKC. The results from this study confirmed our hypothesis that alpha-adrenoceptor signaling may play an important role for arrhythmogenesis under circumstances of catecholamine excess. This information may help clinical doctors to think about application of alpha-blockers for treatment of TTC or heart diseases associated with catecholamine excess, especially when beta-blocker is contraindicated or alone not effective in the treatment.

Although it has been widely accepted that the toxic effects of catecholamine may be a main cause for TTC, other heart diseases may be also influenced by catecholamine effects. It is well-known that catecholamine and adrenoceptor activation may contribute to some heart diseases, likes chronic heart failure, hypertrophic cardiomyopathy, catecholaminergic polymorphic ventricular tachycardia (CPVT), arrhythmogenic right ventricular cardiomyopathy (ARVC), etc. Therefore, the current study may also have implications for those and other cardiac disorders or arrhythmias that are associated with catecholamine effects.

4.3. Conclusion

This study demonstrated that the alpha 1-adrenoceptor signaling is important for the toxic effects of catecholamine excess. High concentration catecholamine can activate alpha 1-receptor besides beta-receptors and cause ion channel dysfunctions, abnormal action potentials and arrhythmias via stimulating ROS and PKC related signaling. This study also suggests that

alpha-blocker can be a possible option for treating arrhythmias in the setting of TTC or other cardiac disorders associated with catecholamine effects.

4.4. Study limitations

Alpha 1-adrenoceptor contains several subtypes such as α_{1A}, α_{1B} und α_{1D}.This study did not clarify which subtype was responsible for observed result.

The study demonstrated that alpha1-receptor activation evoked at least three intracellular signaling, NADPH oxidases, ROS and PKC. Although our data clarified that PKC is a downstream factor of ROS, the alpha1-receptor related signaling responsible for the activation of NADPH oxidases was not revealed. Which factors modulated the Na, Ca and HERG channels were not clarified. In addition, PKC contain more than 10 subtypes. The subtype-specific effects were not investigated, so the subtypes of PKC responsible for the observed effect are unknown.

The hiPSC-CMs possess differences comparing with adult human cardiomyocytes. We cannot rule out the possibility that some intracellular signaling in hiPSC-CMs is different from that in adult human cardiomyocytes. Besides, hiPSC-CMs from TTC-patients were not used for this study. Whether hiPSC-CMs from TTC-patients display different results remain unknown.

The concentration of epinephrine (500 µM) used in this study is much higher than catecholamine concentration in TTC-patients because the sensitivity of hiPSC-CMs to catecholamine is lower than adult human cardiomyocytes. The possibility that native cardiomyocytes differentially response to catecholamine in patients cannot be excluded.

The hiPSC-CMs in this study were derived from only three healthy donors and most experiments were performed in cells from one donor. The possibility that some results may differ in cells from different individuals cannot be rule out.

From a statistical point of view, the results from this study should not be interpreted as that from the whole population, which should be taken into consideration while extrapolating the data.

5. SUMMARY

Takotsubo cardiomyopathy (TTC) is characterized by a transient regional wall motion abnormality with clinical manifestations similar to that of an acute coronary syndrome. Acquired long QT syndrome (LQTs) and life-threatening arrhythmias are common complications of TTC. Both clinical and experimental data suggested an involvement of signaling mediated by non-beta-adrenoceptors in the pathogenesis of TTC. Toxic catecholamine effect has been widely accepted as a main cause for pathogenesis of TTC. Therefore, we investigated the importance of alpha-adrenoceptor related signaling for the toxic effects of catecholamine, focusing on the mechanisms of LQTs and arrhythmias.

Human induced pluripotent stem cell-derived cardiomyocytes (hiPSC-CMs), which were generated from human skin fibroblasts of three healthy donors, were treated with toxic concentration of epinephrine (Epi, 0.5 mM for 1h) or phenylephrine (Pheny, 0.1 mM for 1 h) to mimic the setting of TTC. Different alpha-adrenoceptor agonists and antagonists were used to differentiate receptor-specific effects. Patch clamp, PCR, immunostaining and FACS techniques were employed for the study.

High concentration of epinephrine (Epi) suppressed the depolarization velocity and prolonged the duration (APD) of action potentials (APs) and induced arrhythmic events in hiPSC-CMs. The Epi effects were attenuated by an alpha adrenoceptor blocker (Phentolamine). An alpha 1-adrenoceptor agonist phenylephrine (Pheny) but not an alpha 2-adrenoceptor agonist (clonidine) mimicked Epi-effects on APs, suggesting an involvement of alpha

1-adrenoceptor signaling in APD-prolongation and arrhythmogenesis in the setting of TTC. Epi enhanced ROS-production, which could be attenuated by the alpha-adrenoceptor blocker. Treatment of cells with H_2O_2 (100 μM) mimicked the effects of Epi and Pheny on APs and a ROS-blocker (NAC, 1mM) prevented the Epi and Pheny effects, indicating that the ROS-signaling is involved in the alpha 1-adrenoceptor actions. DPI, an inhibitor of NADPH oxidases blocked the Pheny effects, implying that NADPH oxidases were involved in alpha 1-adrenoceptor signaling. A PKC-blocker (chelerythrine) suppressed the effects of Epi and Pheny, and a PKC stimulator mimicked the effects, implying that PKC participated in alpha 1-receptor signaling. In addition, the PKC-blocker inhibited the effects of H_2O_2, suggesting that PKC acted as a downstream factor of ROS. Epi or Pheny suppressed the peak sodium channel currents and rapidly activating rectifier K currents and enhanced the L-type Ca channel currents, which can explain the abnormal APs induced by alpha 1- adrenoceptor activation.

The study demonstrated that the alpha 1-adrenoceptor signaling plays important roles for ion channel dysfunctions, long QT interval and arrhythmogenesis in the setting of catecholamine excess via α1-adrenoceptor-NADPH-ROS-PKC related signaling. The application of alpha-blocker may be helpful for treating arrhythmias in some patients with TTC or other cardiac diseases associated with toxic catecholamine effects.

6. REFERENCES

1. Sato, H., *Tako-tsubo-like left ventricular dysfunction due to multivessel coronary spasm.* Clinical aspects of myocardial injury: from ischemia to heart failure, 1990: p. 56-64.
2. Sato, H., et al., *Clinical aspect of myocardial injury: from ischemia to heart failure.* Kagaku Hyoronsha, 1990: p. 55-64.
3. Ghadri, J.R., et al., *International Expert Consensus Document on Takotsubo Syndrome (Part I): Clinical Characteristics, Diagnostic Criteria, and Pathophysiology.* Eur Heart J, 2018. **39**(22): p. 2032-2046.
4. Vriz, O., et al., *In-hospital and long-term mortality in Takotsubo cardiomyopathy: a community hospital experience.* J Community Hosp Intern Med Perspect, 2016. **6**(3): p. 31082.
5. Tsuchihashi, K., et al., *Transient left ventricular apical ballooning without coronary artery stenosis: a novel heart syndrome mimicking acute myocardial infarction. Angina Pectoris-Myocardial Infarction Investigations in Japan.* J Am Coll Cardiol, 2001. **38**(1): p. 11-8.
6. Pelliccia, F., et al., *Pathophysiology of Takotsubo Syndrome.* Circulation, 2017. **135**(24): p. 2426-2441.
7. Prasad, A., et al., *Incidence and angiographic characteristics of patients with apical ballooning syndrome (takotsubo/stress cardiomyopathy) in the HORIZONS-AMI trial: an analysis from a multicenter, international study of ST-elevation myocardial infarction.* Catheter Cardiovasc Interv, 2014. **83**(3): p. 343-8.
8. Bybee, K.A., et al., *Clinical characteristics and thrombolysis in myocardial infarction frame counts in women with transient left ventricular apical ballooning syndrome.* Am J Cardiol, 2004. **94**(3): p. 343-6.
9. Redfors, B., et al., *Mortality in takotsubo syndrome is similar to mortality in myocardial infarction - A report from the SWEDEHEART registry.* Int J Cardiol, 2015. **185**: p. 282-9.
10. Deshmukh, A., et al., *Prevalence of Takotsubo cardiomyopathy in the United States.* Am Heart J, 2012. **164**(1): p. 66-71.e1.
11. Templin, C., et al., *Clinical Features and Outcomes of Takotsubo (Stress) Cardiomyopathy.* N Engl J Med, 2015. **373**(10): p. 929-38.
12. Elesber, A., et al., *Myocardial perfusion in apical ballooning syndrome correlate of myocardial injury.* Am Heart J, 2006. **152**(3): p. 469.e9-13.
13. Nef, H.M., H. Mollmann, and A. Elsasser, *Tako-tsubo cardiomyopathy (apical ballooning).* Heart, 2007. **93**(10): p. 1309-15.
14. Konety, S.H., et al., *Arrhythmias in tako-tsubo syndrome--benign or malignant?* Int J Cardiol, 2007. **114**(1): p. 141-4.
15. Wittstein, I.S., *Acute stress cardiomyopathy.* Curr Heart Fail Rep, 2008. **5**(2): p. 61-8.

16. Sharkey, S.W., et al., *Natural history and expansive clinical profile of stress (tako-tsubo) cardiomyopathy.* J Am Coll Cardiol, 2010. **55**(4): p. 333-41.
17. Tornvall, P., et al., *A Case-Control Study of Risk Markers and Mortality in Takotsubo Stress Cardiomyopathy.* J Am Coll Cardiol, 2016. **67**(16): p. 1931-6.
18. Song, B.G., et al., *The impact of stressor patterns on clinical features in patients with tako-tsubo cardiomyopathy: experiences of two tertiary cardiovascular centers.* Clin Cardiol, 2012. **35**(11): p. E6-13.
19. Singh, K., et al., *Meta-analysis of clinical correlates of acute mortality in takotsubo cardiomyopathy.* Am J Cardiol, 2014. **113**(8): p. 1420-8.
20. S, Y.H., *Acute cardiac sympathetic disruption in the pathogenesis of the takotsubo syndrome: a systematic review of the literature to date.* Cardiovasc Revasc Med, 2014. **15**(1): p. 35-42.
21. Ghadri, J.R., et al., *Happy heart syndrome: role of positive emotional stress in takotsubo syndrome.* Eur Heart J, 2016. **37**(37): p. 2823-2829.
22. Wittstein, I.S., et al., *Neurohumoral features of myocardial stunning due to sudden emotional stress.* N Engl J Med, 2005. **352**(6): p. 539-48.
23. Spina, R., et al., *Takotsubo cardiomyopathy following unintentionally large subcutaneous adrenaline injection: a case report.* Eur Heart J Case Rep, 2018. **2**(2): p. yty043.
24. Maes, S., et al., *Takotsubo Cardiomyopathy Induced by Epinephrine Infiltration for Liposuction: Broken Heart Syndrome.* Aesthet Surg J, 2019. **39**(10): p. Np431-np436.
25. Ali, A., et al., *A Case of Takotsubo Cardiomyopathy After Local Anesthetic and Epinephrine Infiltration.* Cureus, 2018. **10**(8): p. e3173.
26. Nazir, S., et al., *Rare case of stress cardiomyopathy due to intramuscular epinephrine administration.* BMJ Case Rep, 2016. **2016**.
27. Paur, H., et al., *High levels of circulating epinephrine trigger apical cardiodepression in a beta2-adrenergic receptor/Gi-dependent manner: a new model of Takotsubo cardiomyopathy.* Circulation, 2012. **126**(6): p. 697-706.
28. S, Y.H. and P. Tornvall, *Epidemiology, pathogenesis, and management of takotsubo syndrome.* Clin Auton Res, 2018. **28**(1): p. 53-65.
29. Sattar, Y., et al., *Management of Takotsubo Syndrome: A Comprehensive Review.* Cureus, 2020. **12**(1): p. e6556.
30. Kato, K., et al., *Takotsubo Recurrence: Morphological Types and Triggers and Identification of Risk Factors.* J Am Coll Cardiol, 2019. **73**(8): p. 982-984.
31. Isogai, T., et al., *Early beta-blocker use and in-hospital mortality in patients with Takotsubo cardiomyopathy.* Heart, 2016. **102**(13): p. 1029-35.
32. Santoro, F., et al., *Lack of efficacy of drug therapy in preventing takotsubo cardiomyopathy recurrence: a meta-analysis.* Clin Cardiol, 2014. **37**(7): p. 434-9.
33. Myagmar, B.E., et al., *Adrenergic Receptors in Individual Ventricular Myocytes: The Beta-1 and Alpha-1B Are in All Cells, the Alpha-1A Is in a*

Subpopulation, and the Beta-2 and Beta-3 Are Mostly Absent. Circ Res, 2017. **120**(7): p. 1103-1115.
34. Ueyama, T., K. Yoshida, and E. Senba, *Stress-induced elevation of the ST segment in the rat electrocardiogram is normalized by an adrenoceptor blocker.* Clin Exp Pharmacol Physiol, 2000. **27**(5-6): p. 384-6.
35. Redfors, B., et al., *Different catecholamines induce different patterns of takotsubo-like cardiac dysfunction in an apparently afterload dependent manner.* Int J Cardiol, 2014. **174**(2): p. 330-6.
36. Kuroda, R., et al., *Immobilization Stress With alpha2-Adrenergic Stimulation Induces Regional and Transient Reduction of Cardiac Contraction Through Gi Coupling in Rats.* Int Heart J, 2015. **56**(5): p. 537-43.
37. Takano, Y., T. Ueyama, and F. Ishikura, *Azelnidipine, unique calcium channel blocker could prevent stress-induced cardiac dysfunction like alpha.beta blocker.* J Cardiol, 2012. **60**(1): p. 18-22.
38. McEntee, R.K., D. Coyle, and M. Meyer, *Severe dilated cardiomyopathy after propranolol treatment in an undiagnosed adrenal pheochromocytoma.* Circ Heart Fail, 2011. **4**(3): p. e10-2.
39. Palecek, T., P. Kuchynka, and A. Linhart, *Treatment of Takotsubo cardiomyopathy.* Curr Pharm Des, 2010. **16**(26): p. 2905-9.
40. Evans, M.J. and M.H. Kaufman, *Establishment in culture of pluripotential cells from mouse embryos.* Nature, 1981. **292**(5819): p. 154-6.
41. Martin, G.R., *Isolation of a pluripotent cell line from early mouse embryos cultured in medium conditioned by teratocarcinoma stem cells.* Proc Natl Acad Sci U S A, 1981. **78**(12): p. 7634-8.
42. Takahashi, K. and S. Yamanaka, *Induction of pluripotent stem cells from mouse embryonic and adult fibroblast cultures by defined factors.* Cell, 2006. **126**(4): p. 663-76.
43. Takahashi, K., et al., *Induction of pluripotent stem cells from adult human fibroblasts by defined factors.* Cell, 2007. **131**(5): p. 861-72.
44. Yu, J., et al., *Induced pluripotent stem cell lines derived from human somatic cells.* Science, 2007. **318**(5858): p. 1917-20.
45. Narazaki, G., et al., *Directed and systematic differentiation of cardiovascular cells from mouse induced pluripotent stem cells.* Circulation, 2008. **118**(5): p. 498-506.
46. Moretti, A., et al., *Patient-specific induced pluripotent stem-cell models for long-QT syndrome.* N Engl J Med, 2010. **363**(15): p. 1397-409.
47. El-Battrawy, I., et al., *Modeling Short QT Syndrome Using Human-Induced Pluripotent Stem Cell-Derived Cardiomyocytes.* J Am Heart Assoc, 2018. **7**(7).
48. Liang, P., et al., *Patient-Specific and Genome-Edited Induced Pluripotent Stem Cell-Derived Cardiomyocytes Elucidate Single-Cell Phenotype of Brugada Syndrome.* J Am Coll Cardiol, 2016. **68**(19): p. 2086-2096.

49. El-Battrawy, I., et al., *Electrical dysfunctions in human-induced pluripotent stem cell-derived cardiomyocytes from a patient with an arrhythmogenic right ventricular cardiomyopathy.* Europace, 2018. **20**(Fi1): p. f46-f56.
50. Acimovic, I., et al., *Post-Translational Modifications and Diastolic Calcium Leak Associated to the Novel RyR2-D3638A Mutation Lead to CPVT in Patient-Specific hiPSC-Derived Cardiomyocytes.* J Clin Med, 2018. **7**(11).
51. Eschenhagen, T. and L. Carrier, *Cardiomyopathy phenotypes in human-induced pluripotent stem cell-derived cardiomyocytes-a systematic review.* Pflugers Arch, 2019. **471**(5): p. 755-768.
52. Qi, C., et al., *The cardioprotective effects of icariin on the isoprenaline-induced takotsubo-like rat model: Involvement of reactive oxygen species and the TLR4/NF-kappaB signaling pathway.* Int Immunopharmacol, 2019. **74**: p. 105733.
53. Borchert, T., et al., *Catecholamine-Dependent beta-Adrenergic Signaling in a Pluripotent Stem Cell Model of Takotsubo Cardiomyopathy.* J Am Coll Cardiol, 2017. **70**(8): p. 975-991.
54. Zhao, Z., et al., *Ion Channel Expression and Characterization in Human Induced Pluripotent Stem Cell-Derived Cardiomyocytes.* Stem Cells Int, 2018. **2018**: p. 6067096.
55. Yücel, G., et al., *Lipopolysaccharides induced inflammatory responses and electrophysiological dysfunctions in human-induced pluripotent stem cell derived cardiomyocytes.* Sci Rep, 2017. **7**(1): p. 2935.
56. El-Battrawy, I., et al., *Hyperthermia Influences the Effects of Sodium Channel Blocking Drugs in Human-Induced Pluripotent Stem Cell-Derived Cardiomyocytes.* PLoS One, 2016. **11**(11): p. e0166143.
57. El-Battrawy, I., et al., *Estradiol protection against toxic effects of catecholamine on electrical properties in human-induced pluripotent stem cell derived cardiomyocytes.* Int J Cardiol, 2018. **254**: p. 195-202.
58. Cai, H., K.K. Griendling, and D.G. Harrison, *The vascular NAD(P)H oxidases as therapeutic targets in cardiovascular diseases.* Trends Pharmacol Sci, 2003. **24**(9): p. 471-8.
59. Lappano, R. and M. Maggiolini, *G protein-coupled receptors: novel targets for drug discovery in cancer.* Nat Rev Drug Discov, 2011. **10**(1): p. 47-60.
60. Kurisu, S., et al., *Tako-tsubo-like left ventricular dysfunction with ST-segment elevation: a novel cardiac syndrome mimicking acute myocardial infarction.* Am Heart J, 2002. **143**(3): p. 448-55.
61. Ako, J., et al., *Transient left ventricular dysfunction under severe stress: brain-heart relationship revisited.* Am J Med, 2006. **119**(1): p. 10-7.
62. Madias, C., et al., *Acquired long QT syndrome from stress cardiomyopathy is associated with ventricular arrhythmias and torsades de pointes.* Heart Rhythm, 2011. **8**(4): p. 555-61.
63. Stiermaier, T., et al., *Prevalence and Clinical Significance of Life-Threatening Arrhythmias in Takotsubo Cardiomyopathy.* J Am Coll Cardiol, 2015. **65**(19): p. 2148-50.

64. Behr, E.R. and S. Mahida, *Takotsubo cardiomyopathy and the long-QT syndrome: an insult to repolarization reserve.* Europace, 2009. **11**(6): p. 697-700.
65. Lindsay, J., et al., *Pathogenesis of the Takotsubo syndrome: a unifying hypothesis.* Am J Cardiol, 2010. **106**(9): p. 1360-3.
66. Lyon, A.R., et al., *Stress (Takotsubo) cardiomyopathy--a novel pathophysiological hypothesis to explain catecholamine-induced acute myocardial stunning.* Nat Clin Pract Cardiovasc Med, 2008. **5**(1): p. 22-9.
67. Heather, L.C., et al., *Isoproterenol induces in vivo functional and metabolic abnormalities: similar to those found in the infarcted rat heart.* J Physiol Pharmacol, 2009. **60**(3): p. 31-9.
68. Mori, H., et al., *Increased responsiveness of left ventricular apical myocardium to adrenergic stimuli.* Cardiovasc Res, 1993. **27**(2): p. 192-8.
69. Lathers, C.M., R.M. Levin, and W.H. Spivey, *Regional distribution of myocardial beta-adrenoceptors in the cat.* Eur J Pharmacol, 1986. **130**(1-2): p. 111-7.
70. Evans, B.A., et al., *Ligand-directed signalling at beta-adrenoceptors.* Br J Pharmacol, 2010. **159**(5): p. 1022-38.
71. Rosenbaum, D.M., S.G. Rasmussen, and B.K. Kobilka, *The structure and function of G-protein-coupled receptors.* Nature, 2009. **459**(7245): p. 356-63.
72. Heubach, J.F., U. Ravens, and A.J. Kaumann, *Epinephrine activates both Gs and Gi pathways, but norepinephrine activates only the Gs pathway through human beta2-adrenoceptors overexpressed in mouse heart.* Mol Pharmacol, 2004. **65**(5): p. 1313-22.
73. Kawakami, K., et al., *Comparison of HERG channel blocking effects of various beta-blockers-- implication for clinical strategy.* Br J Pharmacol, 2006. **147**(6): p. 642-52.
74. Garcia-Elias, A. and B. Benito, *Ion Channel Disorders and Sudden Cardiac Death.* Int J Mol Sci, 2018. **19**(3).
75. Irani, K., *Oxidant signaling in vascular cell growth, death, and survival : a review of the roles of reactive oxygen species in smooth muscle and endothelial cell mitogenic and apoptotic signaling.* Circ Res, 2000. **87**(3): p. 179-83.
76. Tsai, M.H. and M.J. Jiang, *Reactive oxygen species are involved in regulating alpha1-adrenoceptor-activated vascular smooth muscle contraction.* J Biomed Sci, 2010. **17**: p. 67.
77. Nishiura, T. and K. Abe, *Alpha1-adrenergic receptor stimulation induces the expression of receptor activator of nuclear factor kappaB ligand gene via protein kinase C and extracellular signal-regulated kinase pathways in MC3T3-E1 osteoblast-like cells.* Arch Oral Biol, 2007. **52**(8): p. 778-85.
78. Deng, X.F., S. Mulay, and D.R. Varma, *Role of Ca(2+)-independent PKC in alpha 1-adrenoceptor-mediated inotropic responses of neonatal rat hearts.* Am J Physiol, 1997. **273**(3 Pt 2): p. H1113-8.

79. Bayés de Luna, A. and R. Elosua, *Sudden Death.* Revista Española de Cardiología (English Edition), 2012. **65**(11): p. 1039-1052.
80. Tutor, A.S., et al., *Association of 14-3-3 proteins to beta1-adrenergic receptors modulates Kv11.1 K+ channel activity in recombinant systems.* Mol Biol Cell, 2006. **17**(11): p. 4666-74.
81. Urrutia, J., et al., *Mechanisms of IhERG/IKr Modulation by alpha1-Adrenoceptors in HEK293 Cells and Cardiac Myocytes.* Cell Physiol Biochem, 2016. **40**(6): p. 1261-1273.
82. Liu, Y., et al., *Thioridazine Induces Cardiotoxicity via Reactive Oxygen Species-Mediated hERG Channel Deficiency and L-Type Calcium Channel Activation.* Oxid Med Cell Longev, 2020. **2020**: p. 3690123.
83. Aromolaran, A.S., M. Chahine, and M. Boutjdir, *Regulation of Cardiac Voltage-Gated Sodium Channel by Kinases: Roles of Protein Kinases A and C.* Handb Exp Pharmacol, 2018. **246**: p. 161-184.

7. CURRICULUM VITAE

PERSONAL DETAILS

Family name and first name:	Huang, Mengying
Birthday:	16.01.1989
Place of birth:	Sichuan China
Father:	Huang, Qiang
Mather:	Zheng, Hong

SCHOOL EDUCATION

09.2003-07.2006	Yibin No.2 Middle School, Yibin, Sichuan, China

UNIVERSITY EDUCATION

09.2007-06.2012	South West Medical University, China Bachelor of Medicine
09.2014-06.2017	South West Medical University, China Master of Medicine
09.2017-Now	First Department of Medicine, Medical Faculty Mannheim, University of Heidelberg

8. PUBLICATIONS

1.Fanis Buljubasic, Ibrahim El-Battrawy, Huan Lan, Santosh K Lomada, Anupriya Chatterjee, Zhihan Zhao, Xin Li, Rujia Zhong, Qiang Xu, **Mengying Huang**, Zhenxing Liao, Siegfried Lang, Lukas Cyganek, Xiaobo Zhou, Thomas Wieland, Martin Borggrefe, Ibrahim Akin. Nucleoside Diphosphate Kinase B Contributes to Arrhythmogenesis in Human-Induced Pluripotent Stem Cell-Derived Cardiomyocytes from a Patient with Arrhythmogenic Right Ventricular Cardiomyopathy. **Journal of Clinical Medicine**,9(2), 2020.doi: 10.3390/jcm90204862.

2.Ibrahim El-Battrawy, Jonas Müller, Zhihan Zhao, Lukas Cyganek, Rujia Zhong, Feng Zhang, Mandy Kleinsorge, Huan Lan, Xin Li, Qiang Xu, **Mengying Huang**, Zhenxing Liao, Alexander Moscu-Gregor, Sebastian Albers, Hendrik Dinkel, Siegfried Lang, Sebastian Diecke, Wolfram-Hubertus Zimmermann, Jochen Utikal, Thomas Wieland, Martin Borggrefe, Xiaobo Zhou, Ibrahim Akin. Studying Brugada Syndrome with an SCN1B Variants in Human-Induced Pluripotent Stem Cell-Derived Cardiomyocytes. **Frontiers in Cell and Developmental Biology**,11: 261, 2019. doi 10.3389/fcell.2019.00261

3. Zhihan Zhao, Xin Li, Ibrahim El-Battrawy, Huan Lan, Rujia Zhong, Qiang Xu, **Mengying Huang**, Zhenxing Liao, Siegfried Lang, Wolfram-Hubertus Zimmermann, Lukas Cyganek, Thomas Wieland, Ibrahim Akin, Xiao-Bo Zhou and Martin Borggrefe. Drug Testing in Human-Induced Pluripotent Stem Cell–Derived Cardiomyocytes From a Patient With Short QT Syndrome Type 1. **Clinical Pharmacology & Therapeutics**, 106 (3): 642-651,2019. doi：10.1002 / cpt.1449

4. Ibrahim El-Battrawy, Sebastian Albers, Lukas Cyganek, Zhihan Zhao, Huan Lan, Xin Li, Qiang Xu, Mandy Kleinsorge, **Mengying Huang**, Zhenxing Liao, Rujia Zhong, Boris Rudic, Jonas Mueller, Hendrik Dinkel, Siegfried Lang,

Sebastian Diecke, Wolfram-Hubertus Zimmermann, Jochen Utikal, Thomas Wieland, Martin Borggrefe, Xiaobo Zhou, and Ibrahim Akin. A cellular model of Brugada syndrome with SCN10A variants using human-induced pluripotent stem cell-derived cardiomyocytes. **Europace**, 21: 1410–1421,2019. doi:10.1093/europace/euz122

9. ACKNOWLEDGEMENTS

During the study and research in Mannheim Medical Faculty of Heidelberg University, I was very honored to meet my supervisors and friends. This experience is also unforgettable in my life. Here I would like to express frankly my gratitude to all who helped me during my study and during the writing of this thesis.

First of all, I would like to extend my sincere gratitude to my supervisor, Prof. Borggrefe, who invited me and give me the chance to study in Heidelberg University as a doctoral student. I am also very grateful to him for his help and support during my study.

Second, I would like to express my deepest and foremost gratitude to my second supervisor, Dr. Xiaobo Zhou, for his constant encouragement and guidance. He has helped me through all the stages of my experiments and the writing of this thesis. Without his instruction, my experimental research and this thesis could not reach the present level.

Furthermore, I would like to thank my colleagues and friends, Lang Siegfried, Claudia Liebetrau, Ibrahim El-Battrawy, Fanis Buljubasic, Goekhan Yuecel, Katherine Sattler, Zhihan Zhao, Xin Li , Huan Lan, Zhenxing Liao, Qiang Xu, Rujia Zhong, Lin Qiao, Zhen Yang, Yingrui Li, Xuehui Fan, Angela Wendel, who kindly and warmly shared their rich experience and knowledge with me and helped me a lot during my research.

Besides, I am deeply grateful to my parents and my family. Without their love and support, I could not complete my study successfully. Many thanks to their care and support.

Lastly, I would like to thank the Chinese Scholarship Council (CSC) for the financial support for me.